HIAS-E-143

Quantifying the Mortality Consequences of Climate Change: Evidence from Japan

Hongming Wang

Hitotsubashi University

April 15, 2025

Hitotsubashi Institute for Advanced Study, Hitotsubashi University
2-1, Naka, Kunitachi, Tokyo 186-8601, Japan
tel:+81 42 580 8668 http://hias.hit-u.ac.jp/

HIAS discussion papers can be downloaded without charge from:
https://hdl.handle.net/10086/27202
https://ideas.repec.org/s/hit/hiasdp.html

Quantifying the Mortality Consequences of Climate Change: Evidence from Japan*

Hongming Wang†

Hitotsubashi University

April 15, 2025

Abstract

Climate change is projected to increase global temperature and bring about more frequent and intense extreme events including compound extreme events with especially large damage to communities. This paper examines the mortality consequences of climate change across 22 climate change indicators that capture not only shifts in the mean and extremes of weather conditions, but also the amplification of weather extremes when they co-occur and interact in compound extreme events. Using data from 1718 Japan municipalities in 1980-2019, I identify the leading climate drivers of mortality in Japan and quantify the climate-mortality relationship drawing on model specifications selected by LASSO. In addition to temperature, relative humidity, precipitation, and humidity amplification in heat-and-humidity extremes all have significant impacts on mortality, with larger, non-linear effects at the heat extremes of the temperature distribution and both high and low extremes of relative humidity. The mortality responses to heat are concentrated in urban municipalities with no evidence of adaptation between early and late periods of climate change, whereas the mortality responses to humidity amplification are stronger in rural municipalities and fully concentrated in the early period of climate change. Over the study period in 1980-2019, the average municipality in Japan experienced a cumulative mortality of 120 deaths per 10,000 individuals from climate change, of which increases in temperatures contributed 129 deaths, increases in humidity amplification contributed 26 deaths, reductions in precipitation contributed 7 deaths, and reductions in relative humidity lowered mortality by 43 deaths.

Keywords: climate change, mortality risk, population health, Japan
JEL classification: I14, Q51, Q54

*The author acknowledges financial support from the Japan Society for the Promotion of Science (KAKENHI #23K12463). The financial support did not influence the data collection, research method, or the results obtained in this study. The author declares no conflict of interests.

†Address: Room 108, Annex to the Main Building, Hitotsubashi University, 2-1 Naka, Kunitachi, Tokyo, 186-8601, Japan. Email: hongming.wang1@outlook.com

1 Introduction

In 2024, the global average temperature reached 15.1 degrees Celsius, making 2024 the hottest year since 1850 and the first year with an average temperature exceeding the pre-industrial level by more than 1.6 degrees.[1,2] Since 1850, the global average temperature has increased by around 0.06 degrees per decade, but the rate of warming has been three times as fast in the past few decades, reaching an alarming 0.20 degrees per decade since the 1980s.[3] Based on the recent warming rate, it may take less than a decade before the Earth's long-term average temperature reaches 1.5 degrees above the pre-industrial level, beyond which further warming could have irreversible and devastating impacts on human and natural systems (Allen *et al.* 2018; Armstrong McKay *et al.* 2022; Bevacqua *et al.* 2025).

While rising temperature has been the focal point of policy, climate change has also brought about more frequent and more intense extreme weather events affecting precipitation, droughts, humidity, and wind speed. Even absent dramatic increases in temperature, strong winds and more extreme precipitations could elevate flood risks (Davenport *et al.*, 2021), erode soil (Borrelli *et al.*, 2020), and destroy crops (Ortiz *et al.*, 2022), whereas droughts and uncomfortable humidity levels could lead to conflicts, malnutrition, and diseases (Von Uexkull *et al.* 2016; Cooper *et al.* 2019; Colón-González *et al.* 2021). Moreover, multiple extreme and less-than-extreme weather events could occur simultaneously or successively in compound events (CE) and cause enormous damage to environments (AghaKouchak *et al.* 2020; Zscheischler *et al.* 2020). CEs such as hot-and-dry conditions and tropical cyclones are projected to become more frequent under climate change, posing serious threats to agricultural production and infrastructure resilience across wide regions of the world (Knutson *et al.* 2020; Ridder *et al.* 2020).

[1]Copernius Global Climate Highlights 2024: https://climate.copernicus.eu/copernicus-2024-first-year-exceed-15degc-above-pre-industrial-level

[2]Berkeley Temperature Report for 2024: https://berkeleyearth.org/global-temperature-report-for-2024/

[3]NOAA Understanding Climate: https://www.climate.gov/news-features/understanding-climate/climate-change-global-temperature

This paper studies the relationship between climate change and the mortality risk of human populations across 1718 municipalities in Japan over the period 1980-2019. While the previous literature has primarily focused on the temperature as the key driver of climate-related deaths, this paper examines the mortality consequences of a rich set of climate change indicators that capture not only shifts in the mean and extremes of weather conditions, but also the interactive effects when multiple weather extremes co-occur and amplify one another. Specifically, the climate change indicators capture changes in the mean daily air temperature, precipitation, humidity, and wind speed relative to the climatology mean in 1951-1980, changes in the extremes of these weather conditions, as well as changes in the compound extremes across the weather conditions. Weather extremes are identified relative to the 90th and 10th percentile of climatology, and the magnitude of the extreme is measured using the amount of exceedance over the relevant threshold. For co-occurring heat-and-humid extremes, I calculate the heat index from air temperature and relative humidity as a measure of humid heat stress (Steadman, 1979) and use the exceedance of heat index above air temperature to quantify the humidity amplification on hot summer days. On cold winter days, I calculate the wind-chill temperature for cold and windy conditions (Osczevski and Bluestein, 2005) and use the exceedance of wind-chill temperature below air temperature to quantify the amplification from high winds. To measure concurrent precipitation-temperature and precipitation-wind extremes, I follow the literature on climate extreme indices (Tank *et al.* 2009; Zhang *et al.* 2011) and count the number of days when both weather conditions exceed the relevant thresholds. Finally, I use the cumulative sum of exceedances over an uninterrupted series of extreme weather days to capture the temporal compounding in consecutive extremes. For heatwaves, for instance, this measure implies greater exceedances and hence greater discomfort suffered towards later days of the series (Miller *et al.*, 2021).

To quantify the relationship between climate change as captured by the climate change indicators and mortality, the empirical analysis needs to address two main challenges. The

first one is model selection. Assuming that the researcher has included all the relevant climate change indicators in the regression model, the functional form in which the indicators enter the climate-mortality relationship is unknown to the researcher. Instead of assuming linear effects of climate on mortality, one might postulate that larger shifts in weather will lead to disproportionately larger responses in mortality and hence include higher-order terms of climate in the regression model. In addition, if the effects of certain weather extremes are heterogeneous across mean weather conditions within a year or the presence of alternative weather extremes that provide relief, then a more flexible model which also controls for two-way interactions across climate change indicators might be appropriate. When the true model implies zero or near-zero coefficients for most variables in the specified model, results from ordinary least squares (OLS) would contain false positives and large biases compared to the true model. The second challenge is that it is difficult to causally interpret OLS estimates when the model controls for the full set of climate change indicators and their transformations, many of which by construction exhibit high degrees of correlation with one another. In particular, the correlation coefficients between the mean weather and extremes all exceed 0.80 for temperature, humidity, and precipitation. While the correlation improves in-sample fit, it complicates the interpretation of marginal effects when multiple indicators shift in response to a given variation in weather.

To tackle these challenges (i.e., model selection and over-fitting), I apply LASSO as a shrinkage technique to select the key climate change indicators across three specifications of the climate-mortality relationship. In the first, basic specification, I regress municipality-level mortality rates on the climate change indicators without introducing higher-order terms or interactions between indicators. In the second specification, I regress mortality rates on a quadratic functional form that also includes the squared term of each indicator. In the third, fully flexible specification, I regress mortality rates on a quadratic form that further includes the two-way interactions across all climate change indicators. I control for municipality fixed effects in all specifications to ensure that the climate-mortality

relationship is identified from within-municipality, inter-annual variations in weather, thus removing biases from time-invariant, municipality-level confounds such as geography and climate. I cluster the standard errors at the level of municipalities, and set the penalty of the LASSO estimator based on the theoretical results in Belloni *et al.* (2012), which corrects for the dependence structure of the error term when computing the optimal penalty. Across specifications, the LASSO estimator consistently identifies four key climate change indicators that drive mortality in Japan: mean daily air temperature, humidity amplification on hot days, mean daily precipitation, and low humidity extremes. In the quadratic specification, the squared term of mean daily air temperature is selected by the LASSO estimator rather than the linear term. In the fully flexible specification, both mean daily air temperature and mean daily humidity interact significantly with humidity amplification, indicating heterogeneous impacts of compound extremes across different mean weather conditions around the year.

Based on the model selection results from LASSO, my preferred regression specification controls for the linear and squared terms of four climate variables: mean daily air temperature, humidity amplification, mean daily precipitation, and mean daily humidity. The quadratic functional form is widely adopted in the literature to study the impacts of climate on human health and activities (Carleton *et al.* 2022; Hsiang 2016; Burke *et al.* 2015). In this setting, the quadratic form accommodates the non-linear effects of temperature and humidity extremes as indicated by the LASSO estimator.[4] I do not include additional interaction terms in the main analysis for ease of interpretation, but explore differential mortality responses across climate conditions and a rich set of socio-economic characteristics in the heterogeneous analysis. Across time periods, I estimate separate regressions for the early (1980-1999) and later (2000-2019) period of climate change, and compare the marginal responses across periods to understand whether there is adaptation

[4]Most specifications in the literature control for the non-linear effects of temperature and precipitation, but do not consider the mortality effects of humidity or amplifying effect it has on heat. To the extent that the omitted weather variables have significant impacts on the outcome of interest, results from specifications controlling for only temperature and precipitation will be biased.

to the climate hazard over time. I also explore regional heterogeneity in the mortality responses running separate regressions by regions.

I find substantially larger effects of warming on mortality at higher temperatures. Increasing air temperature by 0.39 degrees from climatology, or the mean temperature increase across municipalities over the study period, would lead to 1.49 more deaths per 10,000 individuals per year; at 1 degree above climatology, the same temperature increase would have a much larger death toll of 2.69 deaths per 10,000 individuals per year. The non-linear effect corresponds to a marginal response curve with temperature that slopes significantly upwards. Across time periods, marginal responses estimated from early and later periods of climate change are statistically indistinguishable from one another, implying little adaptation to rising temperatures over the study period. Municipalities with a warmer, wetter, and more humid climate, such as those located in the southern regions of Chubu, Kansai, Shikoku, and Kyushu-Okinawa, have steeper marginal response curves and greater mortality increases as temperature rises. Consistent with the literature on urban heat islands (Patz *et al.* 2005; Huang *et al.* 2023), urban municipalities with high population densities and incomes have substantially larger mortality responses to heat. This suggests that greater resources from economic production may not fully offset the death tolls of excessive heat in densely built urban areas. In contrast, municipalities with higher agricultural incomes exhibit smaller mortality responses to heat, suggesting that better adaptation of the agricultural sector may contribute to lowering heat-related deaths in rural areas.

In contrast to temperature, the mortality response to humidity amplification shows evidence of adaptation across early and later periods of climate change. Specifically, increasing humidity amplification by 18.93 degree days from climatology, or the mean increase across municipalities over the study period, would increase mortality by 1 death per 10,000 individuals per year. This effect is fully concentrated in the early 1980-1999 period whereas in the later 2000-2019 period, humidity amplification has no significant

impact on mortality. Across geography, mortality responses are largest in Hokkaido, the northernmost region with the coldest climate and lowest level of humidity amplification in the climatology baseline. This suggests that humidity amplification could be most lethal where it is least anticipated and where residents are ill-adapted to its effects on health. Moreover, consistent with greater risks of heat-related deaths and morbidity in older ages, municipalities with a higher share of elderly individuals have greater mortality responses to both heat and humidity amplification. However, different from the heat island effect in urban settings, rural, rather than urban, municipalities have larger mortality responses to humidity amplification, and higher agricultural income appears to protect against the mortality effects of humid heat in rural areas.

Across humidity levels, mortality responses are larger at more extreme values of humidity, resulting in a marginal response curve that slopes significantly upwards. In particular, reducing relative humidity by 1.25 percentage points from climatology, or the mean reduction across municipalities over the study period, would lower mortality by 0.95 deaths per 10,000 individuals per year. At lower humidity, however, further reductions would instead increase mortality at humidity extremes. In the warm, southern regions of Kansai and Shikoku, excessively low, rather than high, humidity significantly increases mortality, whereas in Hokkaido, both high and low humidity extremes significantly increase mortality. Across socio-economic characteristics, rural status, low population density, and low agricultural income are all associated with steeper marginal response curves and greater mortality increases at humidity extremes. As with temperature, I do not find evidence of adaptation to humidity across early and later periods of climate change.

Greater precipitation reduces mortality in Japan, with no evidence of statistically different marginal responses across early and later periods of climate change. Reducing precipitation by 0.17 mm/day from climatology, or the mean reduction across municipalities over the study period, would increase mortality by 0.25 deaths per 10,000 individuals per year. The mortality effect is fully concentrated in rural municipalities, whereas in

urban municipalities, reductions in precipitation have no significant impact on mortality. Across geography, mortality responses are larger in the Kansai region as well as the colder regions of Hokkaido and Tohoku, where a 0.17 mm/day reduction in precipitation would increase mortality by 0.48-0.54 deaths per 10,000 individuals per year.

2 Data and Methods

2.1 Constructing the Climate Change Indicators

The climate change indicators are constructed from ERA5-Land, a reanalysis dataset that provides hourly weather data at 0.1°x 0.1°resolutions over the Earth's land surfaces. I focus on grid cells covering Japan and obtain hourly data for air temperature, dewpoint temperature, precipitation, and wind speed from 1950 to 2019. From air and dewpoint temperature, I construct hourly data for relative humidity, and calculate the heat index from air temperature and relative humidity based on the revised Steadman (1979) formula adopted by the NOAA weather service.[5] As the heat index measures the feel-like temperature to human bodies when humidity causes extra discomfort at any given level of heat, I quantify humidity amplification as the difference between the heat index and air temperature when the heat index is higher, and zero otherwise. Similarly, I capture temperatures experienced under cold and windy conditions using the wind-chill temperature (Osczevski and Bluestein, 2005) as adopted by Environment Canada's weather forecast sevices.[6] Wind-chill amplification is quantified as the difference between wind-chill and air temperature when the wind-chill temperature is lower, and zero otherwise.

From the hourly data, I obtain daily air temperature, precipitation, relative humidity, wind speed, humidity amplification, and wind-chill amplification for each day in 1951-

[5]The revised formula is shown at https://www.wpc.ncep.noaa.gov/html/heatindex_equation.shtml

[6]The detailed formula is shown at http://www.med.mcgill.ca/epidemiology/hanley/c609/material/CanadaWindChill.pdf

2019. I define the climatology period as the 30-year period in 1951-1980, and measure climate change in the study period (1980-2019) as shifts relative to the climatology norms in 1951-1980. Specifically, for each day-of-year, the climatology norms consist of the mean and the 10th, 25th, 75th, 90th percentiles of daily weather calculated based on the observed distribution in the climatology period.[7] Weather extremes are identified if the daily weather is above the 90th percentile or below the 10th percentile of climatology, and the magnitude of the extreme is measured using the amount of exceedance of daily weather over the relevant threshold. Because different locations can have drastically different weather conditions and seasons, quantifying weather extremes using the percentile rather than absolute thresholds can flexibly account for the location (at the grid cell level) and seasonal (at the day-of-year level) differences in climate, and hence facilitate the comparison of climate change across locations. To identify concurrent extremes, I adopt less stringent thresholds and require that both weather realizations fall within the top or bottom 25 percent tail of the climatology distribution.

[7] To increase the sample size in the distribution of day-of-year weather, I open a 15-day window around the focal day-of-year and use all days from 7 days before to 7 days after the focal day to determine the climatology means and percentiles.

Table 1: Climate Change Indicators

Indicator	Indicator Name	Description
Weather Mean		
tas	mean daily air temperature	mean daily air temperature in a calendar year (°C)
hmd	mean daily humidity	mean daily relative humidity in a calendar year (%)
precip	mean daily precipitation	mean daily precipitation in a calendar year (mm/day)
sfcWind	mean daily wind speed	mean daily 10m surface wind speed in a calendar year (m/s)
Weather Extremes		
*tas*90*p*	heat extremes	sum of daily temperature exceedances above 90th percentile of climatology
*tas*10*p*	cold extremes	sum of daily temperature exceedances below 10th percentile of climatology
*hmd*90*p*	high humidity extremes	sum of daily humidity exceedances above 90th percentile of climatology
*hmd*10*p*	low humidity extremes	sum of daily humidity exceedances below 10th percentile of climatology
*precip*90*p*	one-day precipitation extremes	sum of wet-day precipitation exceedances above 90th percentile of all wet days in climatology
*dry*10*p*	drought extremes	sum of dryness exceedances below 10th percentile of climatology, with dryness measured using 30-day lagged precipitation
*sfcWind*90*p*	wind extremes	sum of daily wind speed exceedances above 90th percentile of climatology
Concurrent Extremes		
hmdamp	humidity amplification	sum of daily humidity amplification across summer season hot days
windchill	wind-chill amplification	sum of daily wind-chill amplification across winter season cold days
hotwet	hot-and-wet days	number of days with air temperature above 75th percentile and precipitation above 75th percentile
coldwet	cold-and-wet days	number of days with air temperature below 25th percentile and precipitation above 75th percentile
hotdry	hot-and-dry days	number of days with air temperature above 75th percentile and 30-day precipitation below 25th percentile
colddry	cold-and-dry days	number of days with air temperature below 25th percentile and 30-day precipitation below 25th percentile
wetwindy	wet-and-windy days	number of days with precipitation above 75th percentile and wind speed above 75th percentile
drywindy	dry-and-windy days	number of days with 30-day precipitation below 25th percentile and wind speed above 75th percentile
Consecutive Extremes		
heatwave	heatwave heat extremes	sum of daily exposure, where daily exposure is the cumulative sum of heat exceedances in a heatwave
coldspell	cold-spell cold extremes	sum of daily exposure, where daily exposure is the cumulative sum of cold exceedances in a cold spell
wetspell	wet-spell precipitation extremes	sum of daily exposure, where daily exposure is the cumulative sum of precipitation exceedances in a wet spell

Notes: Table lists the 22 climate change indicators and briefly describes their definition. All indicators are at the annual time scale and measured in differences relative to the mean of the same indicator over the climatology period, i.e., anomalies. The indicators are grouped into categories that summarize weather mean (4 indicators), weather extremes (7 indicators), as well as concurrent (8 indicators) and consecutive (3 indicators) extremes. Detailed descriptions of the indicators are provided in the main text.

Table 1 lists the 22 climate change indicators constructed for the study period in 1980-2019. All indicators are at the annual time scale and measured in differences relative to the mean of the same indicator over the climatology period, i.e., anomalies. The first four indicators summarize changes in the mean daily air temperature, precipitation, humidity, and wind speed relative to the mean in climatology. The next set of indicators summarizes changes in the weather extremes, where daily exceedances are summed within year to measure the magnitude of extremes at an annual scale. In particular, to construct an indicator of one-day precipitation extremes ($precip90p$), I identify wet days with precipitation higher than the 90th percentile across all wet days in the grid cell's climatology, and use the sum of wet day exceedances to quantify precipitation extremes in a calendar year. To construct an indicator of drought extremes ($dry10p$), I first construct a daily measure of dryness defined as the precipitation sum over a lagged 30-day period ending on the focal day. Based on the dryness measure, I identify drought days as days with dryness lower than the 10th percentile of climatology.[8] The sum of drought day exceedances indicates the extent of drought extremes in a calendar year.

The next set of indicators summarizes changes in concurrent extremes across temperature, humidity, precipitation, and wind speed. To measure humidity amplification in heat-and-humidity extremes, I focus on the boreal summer (May to October) and use the sum of humidity amplification on heat extreme days (air temperature above 90th percentile of climatology) to quantify the total humidity amplification in a calendar year. I do not also include warmer-than-usual days in the winter season because humidity amplification on heat is minimal in winter with lower absolute temperatures. To measure wind-chill amplification in cold-and-wind extremes, I focus on the boreal winter (November to April) and use the sum of wind-chill amplification across winter season cold days (air temperature below 10th percentile of climatology) to quantify the total wind-chill amplification in a calendar year. For concurrent precipitation-temperature and

[8]This definition of drought days is similar to the SPI measure which identifies drought as a period of low precipitation relative to a fitted distribution from historic records.

precipitation-wind extremes, I adopt the frequency measure from the literature on extreme indices (Tank *et al.* 2009; Zhang *et al.* 2011) and count the number of days when both weather conditions exceed the relevant thresholds. For instance, $hotdry$ indicates changes in the number of hot-and-dry days where air temperature is above the 75th percentile and dryness is below the 25th percentile of climatology.

The final set of indicators summarizes changes in consecutive weather extremes. In such events, a series of calendar days are exposed to a specific type of weather extreme without respite, and due to temporal compounding, discomfort experienced earlier in the event could amplify the discomfort from focal-day extremes. To quantify the temporal compounding, I follow Miller *et al.* (2021) and adopt a simple, additive specification assuming that discomfort builds up and increases focal-day discomfort linearly in consecutive extremes. Under this specification, a daily measure of temporal compounding could be constructed as the cumulative sum of exceedances from the first day of the event up to the day prior to the focal day, with non-event days given a temporal compounding of zero. The daily measures are summed over the summer season, winter season, and wet days to construct indicators of heatwaves, cold spells, and wet spells, respectively, in a calendar year.

2.2 Climate Change as Captured by the Indicators

I aggregate grid cell-level indicators to the level of municipalities and plot the climate change indicators over time in Figure 1.[9] In the panels, each circle represents a municipality in a given year. The red bars show the mean of the indicator across municipalities for each decade of the study period. The blue line shows the smooth time trend of the indicator fitted by lowess. In panel (a), mean daily air temperature shows a substantial

[9] I aggregate the indicators to the municipality level applying area and population weights. I obtain detailed population counts across micro areas, or meshes, from the 2000 Census of Japan. Each mesh is roughly 22.5 seconds in length and 15 seconds in width. The mesh-level population counts are aggregated to the level of 0.1°x 0.1°grid cells and divided by the size of land area in each grid cell to compute the population weights.

upward trend over the study period, increasing from -0.26 degrees in the 1980s to 0.40 degrees in the 1990s, 0.60 degrees in the 2000s, and 0.83 degrees in the 2010s. Against the time trend, there is substantial inter-annual variation in weather, with almost all municipalities experiencing hotter-than-normal temperatures in 1990-1992, 2007-2010, and 2015-2019 and colder temperatures in between. Across temperature extremes, cold extremes and cold spells decreased sharply in the 1980s and 1990s (panel f and u), whereas heat extremes and heatwaves increased more towards the end of the study period in the 2010s (panel e and t).

In panel (b), relative humidity shows a persistent drying trend, decreasing from -0.77 percentage points (pp) in the 1980s to -1.16 pp in the 1990s, -1.46 pp in the 2000s, and -1.62 pp in the 2010s. Consistent with the drop in mean humidity, high humidity extremes decreased in panel (g) whereas low humidity extremes increased sharply in the 1990s, exposing more municipalities to historically dry conditions in 2000-2019 (panel h). Mean daily precipitation similarly shows a small drying trend from 1980 to 2009, with anomalies ranging from -0.22 mm/day in the 1980s to -0.20 mm/day in the 1990s and -0.32 mm/day in the 2000s (panel c). Mean daily precipitation then increased to 0.05 mm/day in the 2010s. One-day precipitation extremes showed a similar increase in the 2010s (panel i), whereas drought extremes began to decline in the 2000s after reaching high levels in the 1990s (panel j). Wet spells did not show significant trending over the sample period (panel v). In panel (k), wind speed extremes increased especially in the later period in 2000-2019, but the change in the mean wind speed was overall small in the study period (panel d).

Across concurrent extremes, humidity amplification in heat-humidity extremes increased roughly linearly over the study period, and more municipalities experienced record high levels of humidity amplification in the late 2010s (panel l). In cold-wind extremes, wind-chill amplification decreased over the study period, and larger reductions were concentrated in the early period in 1980-1999 (panel m). Both cold-and-dry and cold-and-wet extremes decreased over time (panel q and o) whereas hot-and-dry and

Figure 1: Climate Change Indicators, 1980-2019

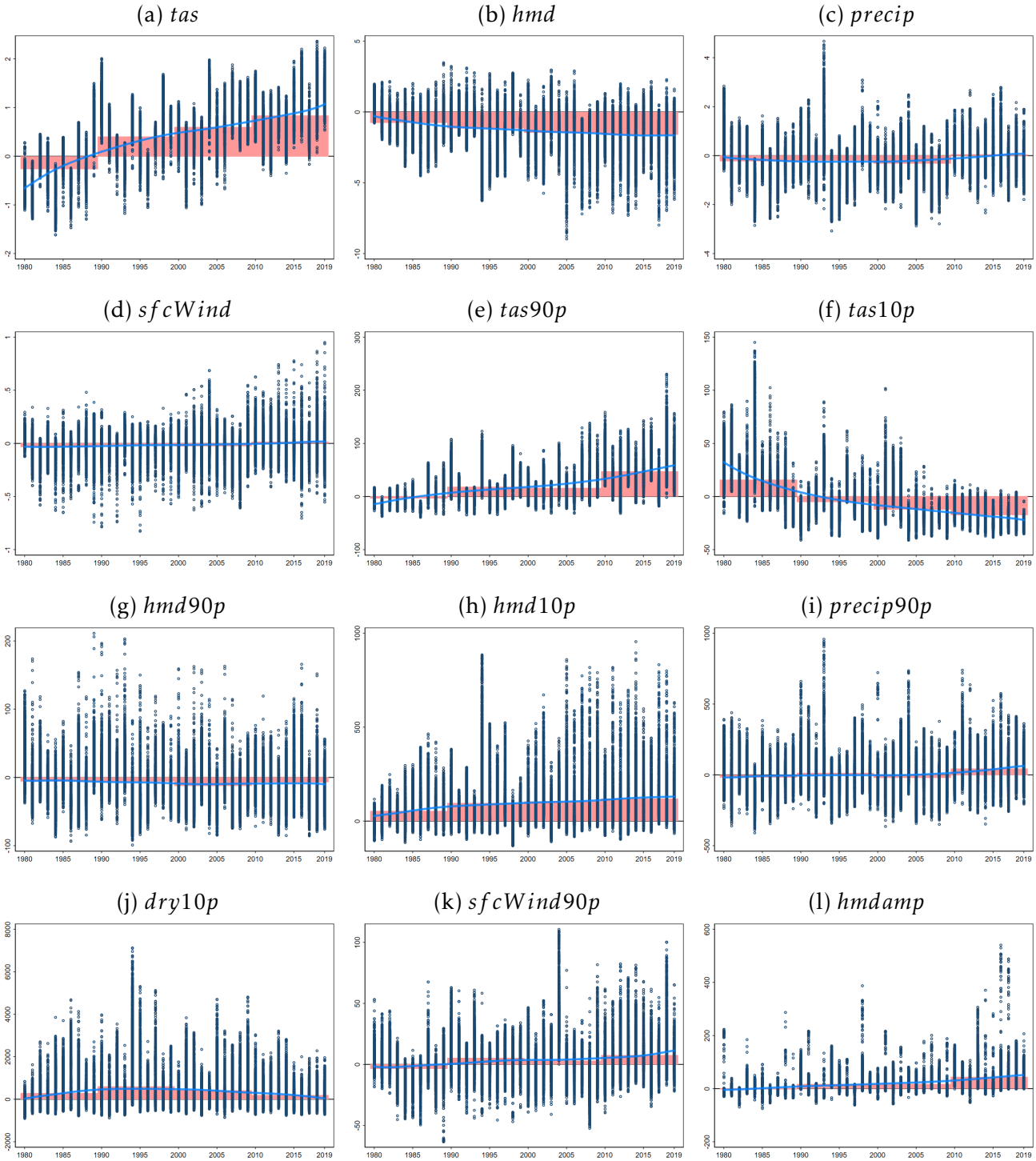

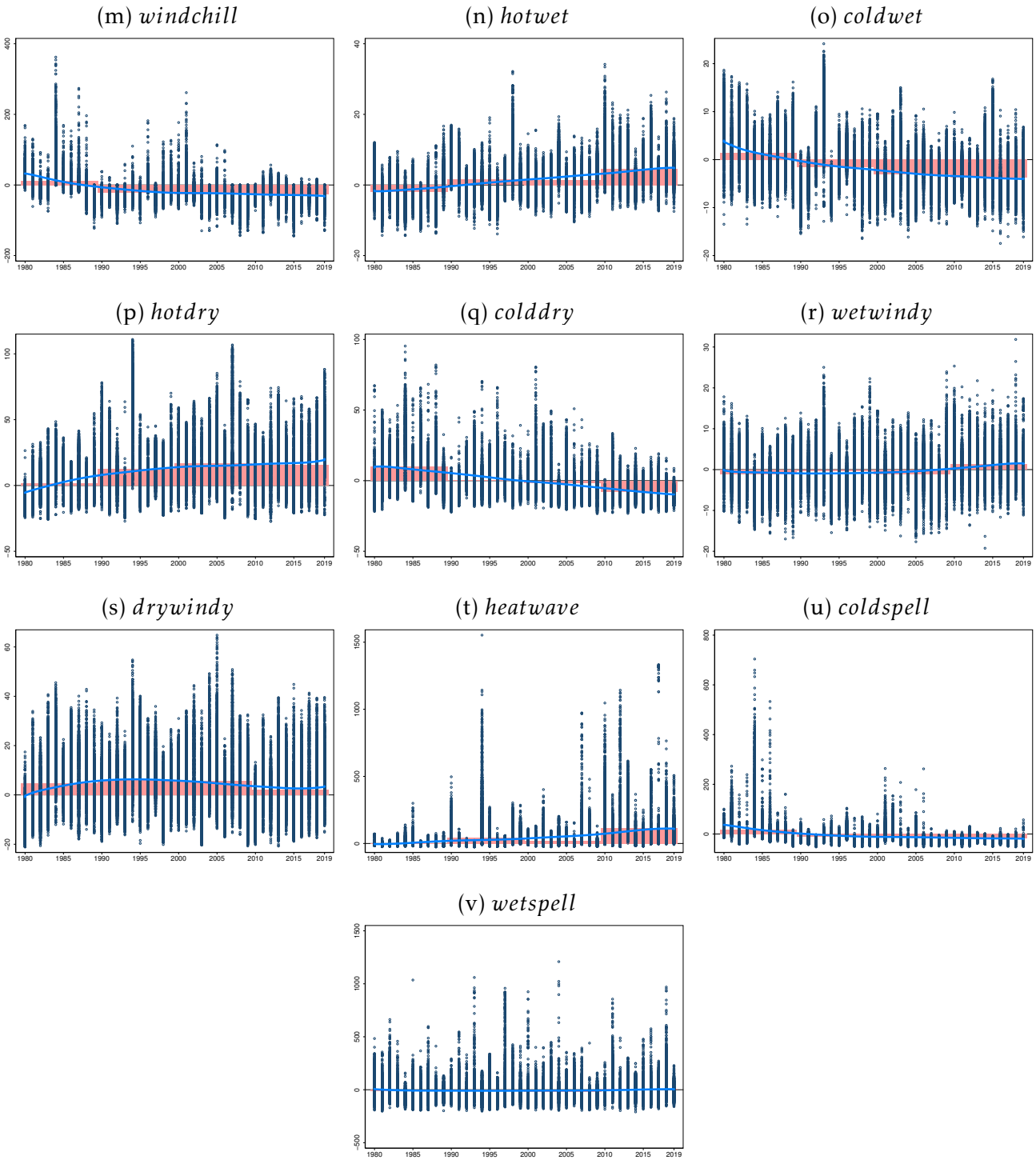

Notes: Figure plots the climate change indicators across municipalities and over time. In the panels, each circle represents a municipality in a given year. The red bars show the mean of the indicator across municipalities for each decade in 1980-2019. The blue line shows the smooth time trend of the indicator fitted by lowess. All indicators are at the annual time scale and measured in differences relative to the mean of the same indicator over the climatology period, i.e., anomalies.

hot-and-wet extremes increased (panel p and n). In particular, hot-and-dry extremes increased significantly in the 1990s and stayed roughly constant in 2000-2019, whereas cold-and-dry extremes decreased throughout the study period. Wet-and-windy extremes increased in the 2010s when both precipitation and wind speed increased compared to earlier periods (panel r). Dry-and-windy extremes were larger in the 1990s and decreased after, matching the trend of dryness over the study period (panel s).

2.3 Empirical Strategy

I next examine the mortality consequences of climate change as captured by the climate change indicators across 1718 Japan municipalities in 1980-2019. Doing so requires addressing two main challenges in this setting. The first one is model selection. Assuming that the set of climate change indicators has sufficiently captured all relevant weather variations that may impact mortality, the functional form in which the indicators enter the true climate-mortality relationship is unknown to the researcher. Instead of assuming linear effects of climate on mortality, for instance, one might postulate that larger shifts in weather will lead to disproportionately larger responses in mortality and hence include higher-order terms of climate in the regression model. In addition, if the effects of certain weather extremes are heterogeneous across mean weather conditions within a year or the presence of alternative weather extremes that provide relief, then a more flexible model which also controls for two-way interactions across climate change indicators might be appropriate. When the true climate-mortality relationship includes only a subset of climate change indicators and their transformations, results from ordinary least squares (OLS) would contain false positives and large biases compared to the true model.

Second, even absent biases from model mis-specification, it is difficult to causally interpret the OLS estimates when regressors exhibit high degrees of correlation with one another. In particular, as shown in Appendix Figure A1, the correlation coefficients between weather mean and extremes are as high as 0.81-0.82 for air temperature, 0.65-

0.85 for humidity, and 0.60-0.81 for precipitation. While the high correlation improves in-sample fit, it complicates the interpretation of marginal effects when multiple indicators shift in response to a given variation in weather.

To tackle the challenges (i.e., model selection and over-fitting), I apply LASSO as a shrinkage technique to select the key climate change indicators across three specifications of the climate-mortality relationship. In the first, basic specification, I regress municipality-level mortality rates on the climate change indicators without introducing higher-order terms or interactions between indicators. Specifically, I estimate the following regression

$$y_{it} = \beta_0 + \sum_{k=1}^{K} \beta_1^k \cdot \mathbb{C}_{it}^k + \phi_i + \psi_{p(i)t} + \epsilon_{it}, \tag{1}$$

where mortality rate y_{it} in municipality i and year t is regressed on the climate change indicators $(\mathbb{C}_{it}^k)_{k=1,\dots,K}$, and β_1^k is the coefficient of the kth indicator. I control for municipality fixed effect ϕ_m to ensure that the marginal effects of the climate change indicators are identified from within-municipality, inter-annual variations in weather. The within comparison removes biases from time-invariant, municipality-specific factors such as geography and climate, which are correlated with the climate change indicators and have independent impacts on mortality. I further control for prefecture-by-year effects $\psi_{p(i)t}$ to capture time-varying factors such as policy changes and technology adoption across Japan prefectures. With these controls, β_1^k's estimate the marginal mortality responses to naturally occurring, stochastic realizations of atmospheric conditions across years.

In the second, quadratic specification, I regress mortality rates on a quadratic functional form that controls for the linear and the squared term of each indicator

$$y_{it} = \beta_0 + \sum_{k=1}^{K} \beta_1^k \cdot \mathbb{C}_{it}^k + \sum_{k=1}^{K} \beta_2^k \cdot \mathbb{C}_{it}^k \cdot \mathbb{C}_{it}^k + \phi_i + \psi_{p(i)t} + \epsilon_{it}. \tag{2}$$

The marginal mortality effect of indicator $\mathbb{C}_{it}^k$ is given by $\beta_1^k + 2\beta_2^k \mathbb{C}_{it}^k$. With $\beta_2^k > 0$, the

marginal mortality effect increases in municipality-years with greater realizations of $\mathbb{C}_{it}^k$.

In the third, fully flexible specification, I regress mortality rates on a quadratic form that further includes the two-way interactions across all climate change indicators

$$y_{it} = \beta_0 + \sum_{k=1}^{K} \beta_1^k \cdot \mathbb{C}_{it}^k + \sum_{k=1}^{K} \beta_2^k \cdot \mathbb{C}_{it}^k \cdot \mathbb{C}_{it}^k + \sum_{k=1}^{K-1} \sum_{l=k+1}^{K} \gamma_{kl} \cdot \mathbb{C}_{it}^k \cdot \mathbb{C}_{it}^l + \phi_i + \psi_{p(i)t} + \epsilon_{it}. \quad (3)$$

The marginal mortality effect of indicator $\mathbb{C}_{it}^k$ is given by $\beta_1^k + 2\beta_2^k \mathbb{C}_{it}^k + \sum_{j=1}^{k-1} \gamma_{jk} \mathbb{C}_{it}^j + \sum_{j=k+1}^{K} \gamma_{kj} \mathbb{C}_{it}^j$, which is heterogeneous across all other indicators through the $\gamma_{k\cdot}$ terms. The heterogeneity with respect to mean weather could arise from an acclimatization effect, if, for instance, higher temperatures in a warm year weaken the mortality impacts of heat extremes in the year. The heterogeneity with respect to alternative weather extremes could arise from compound events where extremes occurring in different seasons of the year interact and cause significant impacts on mortality. For instance, droughts followed by high winds and low humidity could elevate the risk of wildfires, whereas droughts followed by precipitation extremes or wet spells could lead to mud slides and flash floods. The mortality consequences of such consecutive extremes not in the climate change indicators are captured by the flexible interaction terms in equation 3.

I then apply the rigorous LASSO estimator (Belloni *et al.*, 2012) to each of the three specifications to select the key climate change indicators that impact mortality. While the standard LASSO technique is designed for homoskedastic and Gaussian errors (Tibshirani 1996; Bickel *et al.* 2009), the rigorous LASSO estimator generalizes the standard results to cases where the error term is heteroskedastic, non-Gaussian, and cluster-dependent (Belloni *et al.* 2012; Belloni *et al.* 2014; Belloni *et al.* 2016). In particular, Belloni *et al.* (2016) derives optimal penalties for panel data that exhibit within-group correlation and heteroskedasticity. I cluster standard errors at the level of municipalities to allow for serial correlations and use the optimal penalties from Belloni *et al.* (2016) to select the key climate drivers of mortality with rigorous LASSO.

Figure 2 shows the LASSO selected variables across specifications. The plotted coefficients indicate the increase in standard deviations of mortality for a one-standard deviation increase in the selected variables. These coefficients are estimated from a post-LASSO OLS regression where both mortality and the selected variables are normalized in standard deviation units. Based on the magnitude of the coefficients, the selected variables are shown in declining orders of importance in each panel.

In panel (a), mean daily air temperature (*tas*) is the leading driver of mortality under the linear specification, with a one-standard deviation increase in temperature increasing mortality by 1.97 standard deviations. Humidity amplification (*hmdamp*) in heat-and-humid extremes also has significant impacts on mortality, with a one-standard deviation increase in humidity amplification increasing mortality by 1.16 standard deviations. The third indicator selected is mean daily precipitation (*precip*). According to the estimate, reducing mean daily precipitation by one standard deviation would increase mortality by 0.94 standard deviations. The fourth variable selected is low humidity extreme ($hmd10p$). For a one-standard deviation increase in low humidity extreme, mortality would increase by 0.36 standard deviations, and the effect is only marginally significant.

In panel (b), the same set of climate change indicators are also selected under the quadratic specification, with the key difference that mean daily air temperature (*tas*) enters via the squared term rather than the linear term in the quadratic specification. Both increases in mean temperature and humidity amplification significantly increase mortality to a similar extent. Increases in mean daily precipitation (*precip*) significantly decrease mortality whereas low humidity extremes ($hmd10p$) increase mortality, and the effects are comparable to those estimated under the linear specification in panel (a).

In panel (c), consistent with results from the linear and quadratic specifications, the leading climate driver across the climate change indicators and their two-way interactions is $tas \cdot hmdamp$. This implies that years with higher mean daily temperature and higher humidity amplification have significantly larger mortality rates, with a one-standard

Figure 2: Mortality impacts of LASSO-selected climate change indicators

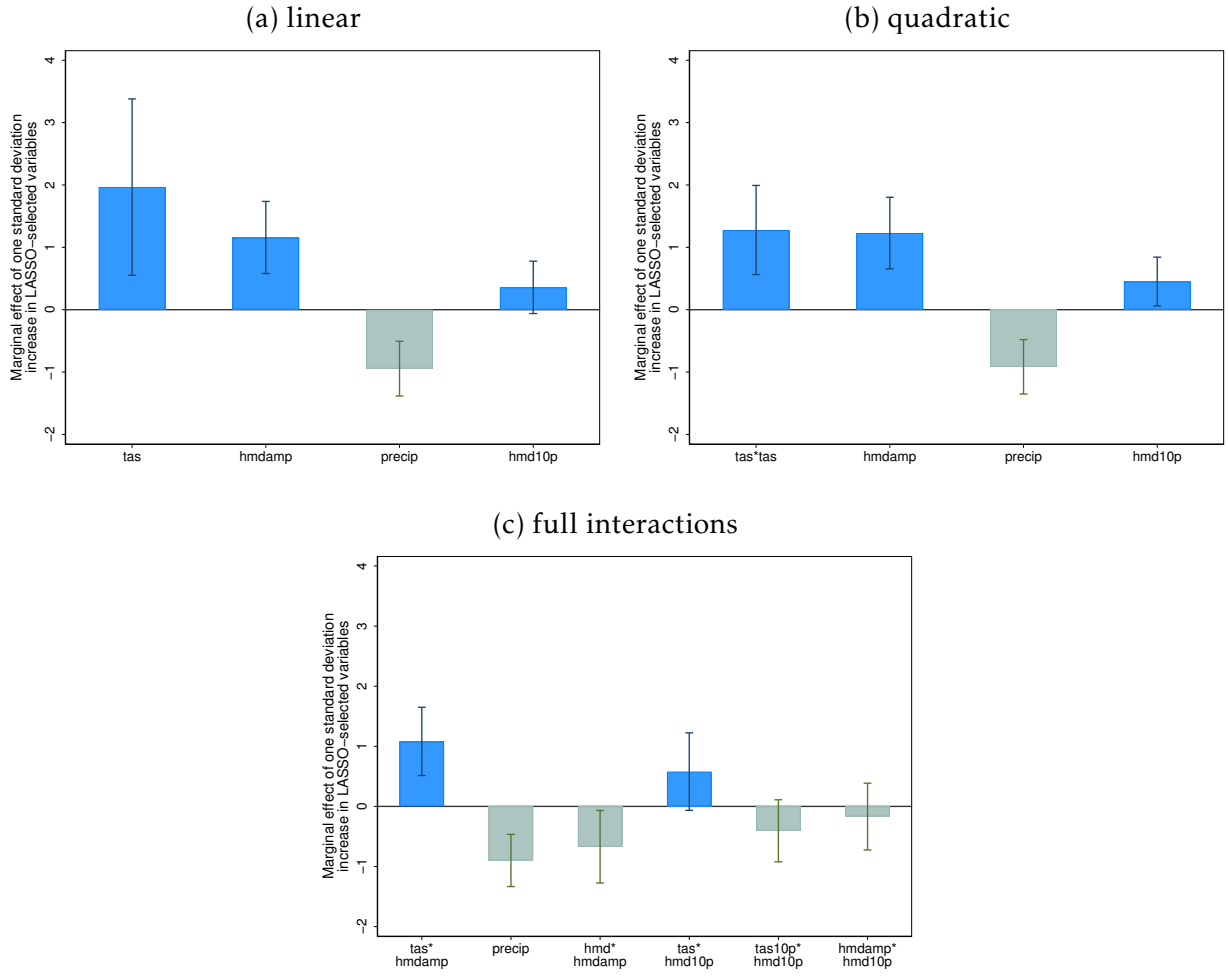

Notes: Figure shows the climate change indicators selected by the rigorous LASSO estimator when the regression model assumes a liner (panel a), quadratic (panel b) and a fully flexible function form including all two-way interactions across the climate change indicators (panel c). The coefficients in each panel are estimated from post-LASSO OLS regressions where both mortality and the selected variables are normalized in standard deviation units. Based on the magnitude of the coefficients, the selected variables are shown in declining orders of importance in each panel. 95% confidence intervals from standard errors clustered at the level of municipalities are shown with the point estimates.

deviation increase in this variable associated with a 1.08 standard deviation increase in mortality. In addition, mean daily humidity interacts significantly with humidity amplification in the variable $hmd \cdot hmdamp$, which has a negative effect on mortality. The negative effect might suggest greater adaptation to humid heat stress in years that are more humid on average, possibly due to acclimatization to the mean. Moreover, years with lower precipitation ($precip$) and hot-and-dry years with high temperatures and low humidity ($tas \cdot hmd10p$) tend to have significantly larger mortality, consistent with results from the linear and quadratic specifications, whereas the mortality difference in cold-and-dry years ($tas10p \cdot hmd10p$) is not statistically significant.

Based on the model selection results, in my preferred specification, I control for the linear and squared terms of four key climate change indicators identified by LASSO: mean daily air temperature tas, total humidity amplification $hmdamp$, mean daily relative humidity hmd, and mean daily precipitation $precip$. Specifically, I estimate the following regression

$$y_{it} = \beta_0 + \beta_1 \cdot tas_{it} + \beta_2 \cdot tas_{it}^2 + \beta_3 \cdot hmdamp_{it} + \beta_4 \cdot hmdamp_{it}^2 + \beta_5 \cdot hmd_{it} + \beta_6 \cdot hmd_{it}^2 \quad (4)$$
$$+ \beta_7 \cdot precip_{it} + \beta_8 \cdot precip_{it}^2 + \phi_i + \psi_{p(i)t} + \epsilon_{it}.$$

The quadratic specification is widely adopted in the climate literature to study the impacts on human health and activities (Carleton *et al.* 2022; Hsiang 2016; Burke *et al.* 2015). In this setting, the quadratic form accommodates the non-linear effects of temperature and humidity extremes as indicated by LASSO. I do not include additional interaction terms in the main analysis for ease of interpretation, but explore differential mortality responses across climate conditions and a rich set of socio-economic characteristics in the heterogeneous analysis. Across time periods, I estimate separate regressions for the early (1980-1999) and later (2000-2019) period of climate change, and compare the marginal responses across periods to understand whether there is adaptation to the climate hazards

over time. I also explore regional heterogeneity in the mortality responses running separate regressions by regions. A map of the climate change indicators across 1718 municipalities in Japan is shown in Appendix Figure A2. A map of the baseline climate characterized by the climatology mean of the indicators is shown in Appendix Figure A3.

3 Results

3.1 Mortality effects of climate change

Figure 3 shows the relationship between mortality and anomalies in mean daily air temperature as based on the quadratic specification in equation 4. In panel (a), predicted mortality increases sharply with temperature in the heat extreme. Compared to mortality at the climatology mean (95.09 deaths per 10,000 individuals), a 0.5 degree increase in temperature would increase mortality to 97.38 deaths per 10,0000 individuals, and a 1.5 degree increase would further increase it to 104.27 deaths per 10,000 individuals. By contrast, mortality is much less responsive to temperature in the cold extreme. The non-linear relationship corresponds to a marginal response curve in panel (b) that slopes significantly upwards with temperature. Specifically, the marginal effects on mortality are small and insignificant at lower temperatures but increase significantly with higher temperatures in the heat extreme. Based on the estimated effects, increasing air temperature by 0.39 degrees from climatology, or the average temperature increase across municipalities over the study period, would lead to 1.49 more deaths per 10,000 individuals per year. At 1 degree above climatology, however, the same temperature increase would lead to a much larger death toll of 2.69 deaths per 10,000 individuals per year.

Panel (c) shows the mortality-temperature relationship separately for the early (1980-1999) and late (2000-2019) period of climate change. While predicted mortality is greater in level in the later period, the slopes of predicted mortality with respect to temperature anomalies are comparable across periods. In panel (d), the marginal response curves from

both periods are statistically indistinguishable from one another, indicating no significant differences in the mortality responses across the range of temperature anomalies observed in both periods. Across temperature anomalies frequently observed in both periods (0 to 1 degree increase), the marginal responses are nearly identical. This suggests that adaptation to heat has been minimal during the study period despite substantially larger temperature increases in the later period.

Unlike temperature, the mortality response to humidity amplification shows evidence of adaptation across early and later periods of climate change. In Figure 4, predicted mortality increases sharply with humidity amplification in the early period but is flat across the full range of humidity amplification in the later period (panel c and d). As large increases in humidity amplification (above 300 degree days per year) are almost entirely concentrated in the later period, the relationship from pooled regressions indicates a drop in predicted mortality and negative marginal effects at large anomalies of humidity amplification (panel a and b), where the mortality effects are much smaller in the later compared to the early period. Based on the pooled estimate in panel (b), increasing humidity amplification by 18.93 degree days from climatology, or the average increase across municipalities over the study period, would increase mortality by 1 death per 10,000 individuals per year.

In Figure 5, mortality increases non-linearly at both high and low extremes of relative humidity, resulting in a marginal response curve that slopes significantly upwards (panel a and b). According to the marginal effects in panel (b), reducing relative humidity by 1.25 percentage points from climatology, or the average reduction across municipalities over the study period, would lower mortality by 0.95 deaths per 10,000 individuals per year. A similar reduction from 6 percentage points below climatology, however, would instead increase mortality by 0.51 deaths per 10,000 individuals per year. In panel (c), the mortality-humidity relationships are fairly comparable across periods, with somewhat larger responses at low humidity extremes in the early as compared to the later period.

However, differences in the marginal responses are not statistically significant in panel (d).

In Figure 6, greater precipitation generally reduces mortality in Japan, and the marginal response curve is roughly constant across the range of precipitation anomalies observed in sample (panel a and b). Applying the marginal effects, reducing precipitation by 0.17 mm/day from climatology, or the average reduction across municipalities over the study period, would increase mortality by 0.25 deaths per 10,000 individuals per year. Comparing early and late periods, the mortality-precipitation relationships are virtually identical across the range of anomalies observed in both periods, and differences in the marginal responses are not statistically significant (panel c and d).

3.2 Heterogeneity by geography

I next explore heterogeneous effects across 8 regions in Japan with separate regressions in each region. In Figure 7, the mortality response to temperature is largest in the southern-central region of Kansai, which includes the prefectures of Hyōgo, Kyōto, Mie, Nara, Ōsaka, Shiga, and Wakayama. In this region, increasing mean daily temperature by 1 degree from the climatology would lead to 15.43 more deaths per 10,000 individuals per year. In addition to Kansai, the central region of Chubu and the southern regions of Shikoku and Kyushu-Okinawa also show large mortality increases with temperature.

In Figure 8, the mortality responses to humidity amplification are larger in the northernmost region of Hokkaido, where the climate is coldest and humidity amplification is lowest in the climatology baseline, and in the southern-central regions of Chubu, Kansai, and Chugoku. In Hokkaido, a 1 degree-day increase in humidity amplification would lead to 0.27 more deaths per 10,000 individuals per year. In the southern-central regions, a similar increase would lead to 0.085-0.13 more deaths per 10,000 individuals per year.

In Figure 9, mortality increases significantly at both high and low humidity extremes in the northernmost region of Hokkaido, whereas in the southern-central region of Kansai and the southern region of Shikoku, mortality tends to decrease at low, rather than high,

Figure 3: Effects of mean daily air temperature on mortality

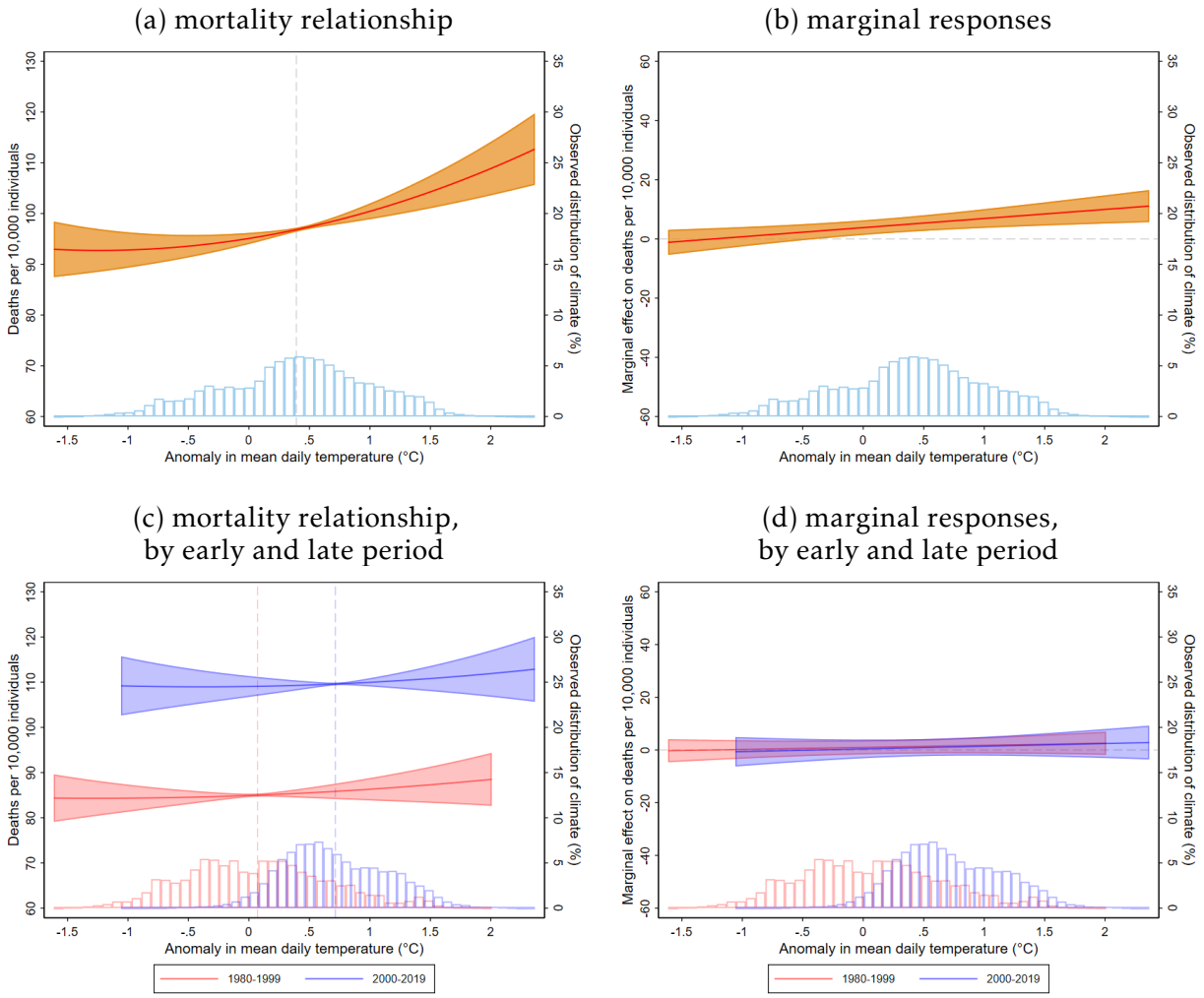

Notes: Figure shows the relationship between mortality and mean daily air temperature as estimated by the quadratic specification in equation 4. Panel (a) plots predicted mortality for air temperature anomalies ranging from the minimum to the maximum in the estimation sample, and panel (b) plots the marginal responses. The empirical distribution of the anomalies observed over the study period is shown in the histogram in light blue. Panel (c) and (d) plot the predicted mortality and the marginal responses separately for the early (1980-1999) and late (2000-2019) periods of climate change, with the empirical distribution of climate anomalies in each period shown in histograms. The dotted vertical lines mark the mean anomaly in the full sample and in each sub-period. 95% confidence intervals from standard errors clustered at the level of municipalities are shown for the predicted mortality and marginal responses.

Figure 4: Effects of humidity amplification on mortality

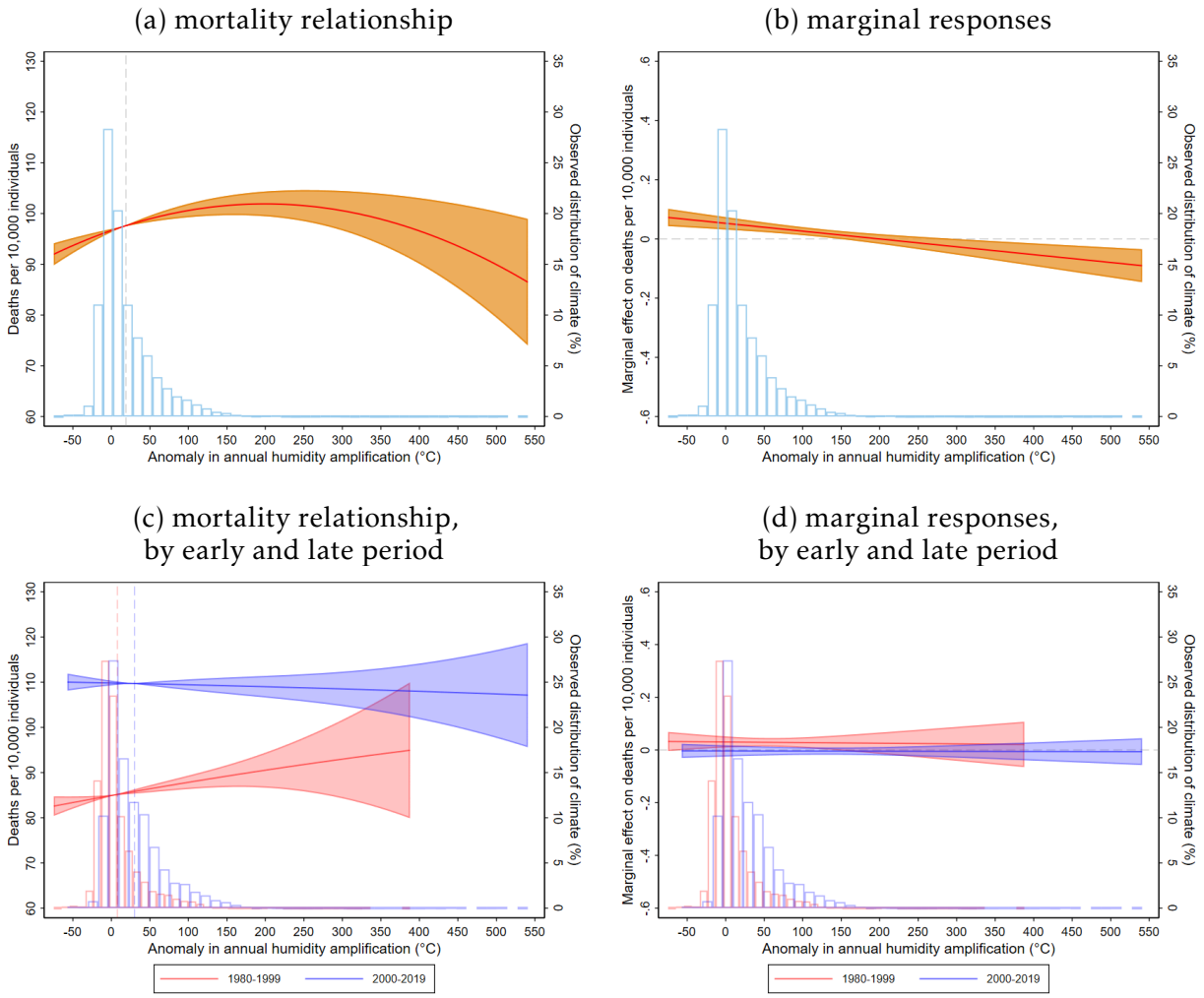

Notes: Figure shows the relationship between mortality and humidity amplification as estimated by the quadratic specification in equation 4. Panel (a) plots predicted mortality for humidity amplification anomalies ranging from the minimum to the maximum in the estimation sample, and panel (b) plots the marginal responses. The empirical distribution of the anomalies observed over the study period is shown in the histogram in light blue. Panel (c) and (d) plot the predicted mortality and the marginal responses separately for the early (1980-1999) and late (2000-2019) periods of climate change, with the empirical distribution of climate anomalies in each period shown in histograms. The dotted vertical lines mark the mean anomaly in the full sample and in each sub-period. 95% confidence intervals from standard errors clustered at the level of municipalities are shown for the predicted mortality and marginal responses.

Figure 5: Effects of mean daily relative humidity on mortality

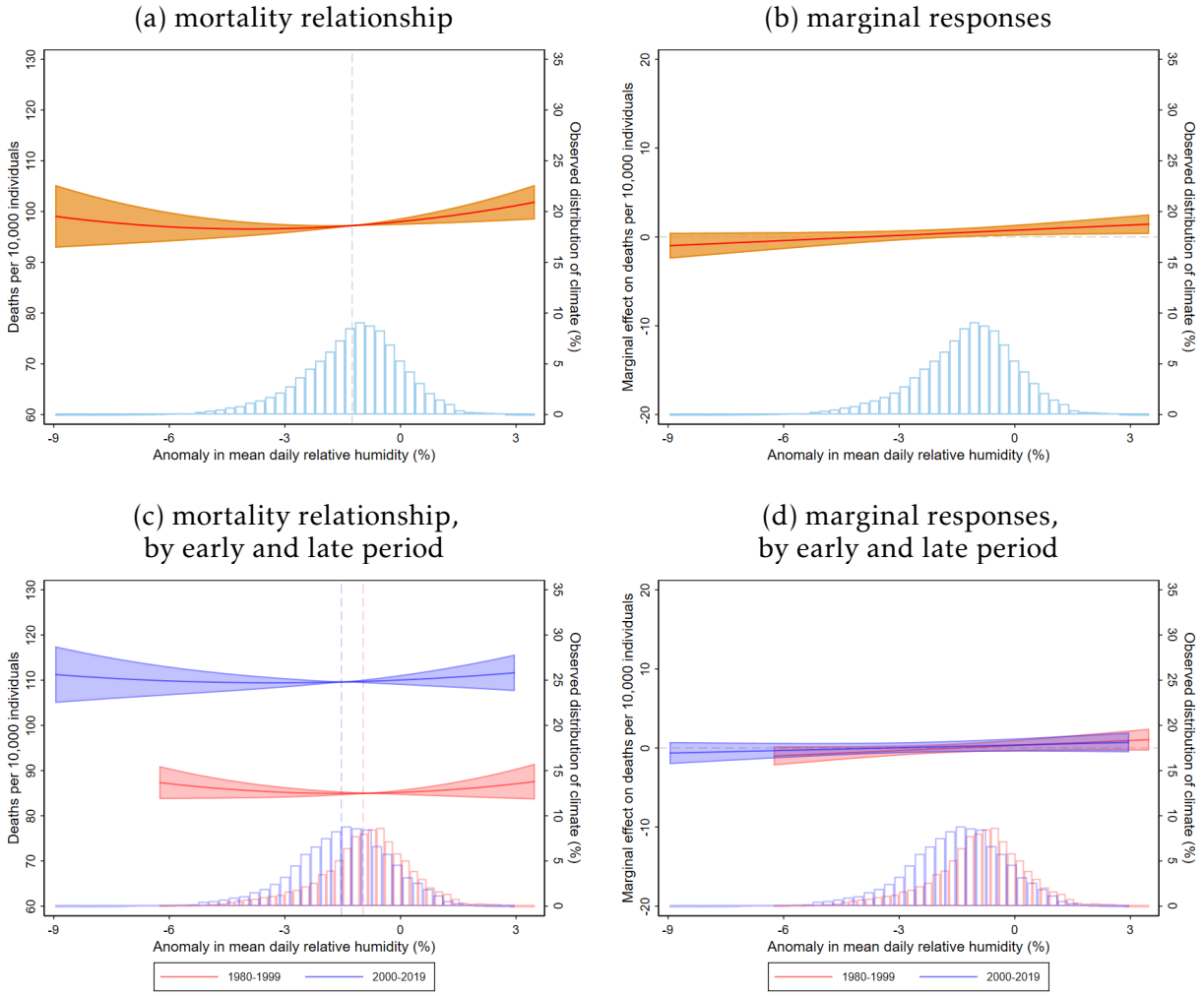

Notes: Figure shows the relationship between mortality and mean daily relative humidity as estimated by the quadratic specification in equation 4. Panel (a) plots predicted mortality for humidity anomalies ranging from the minimum to the maximum in the estimation sample, and panel (b) plots the marginal responses. The empirical distribution of the anomalies observed over the study period is shown in the histogram in light blue. Panel (c) and (d) plot the predicted mortality and the marginal responses separately for the early (1980-1999) and late (2000-2019) periods of climate change, with the empirical distribution of climate anomalies in each period shown in histograms. The dotted vertical lines mark the mean anomaly in the full sample and in each sub-period. 95% confidence intervals from standard errors clustered at the level of municipalities are shown for the predicted mortality and marginal responses.

Figure 6: Effects of mean daily precipitation on mortality

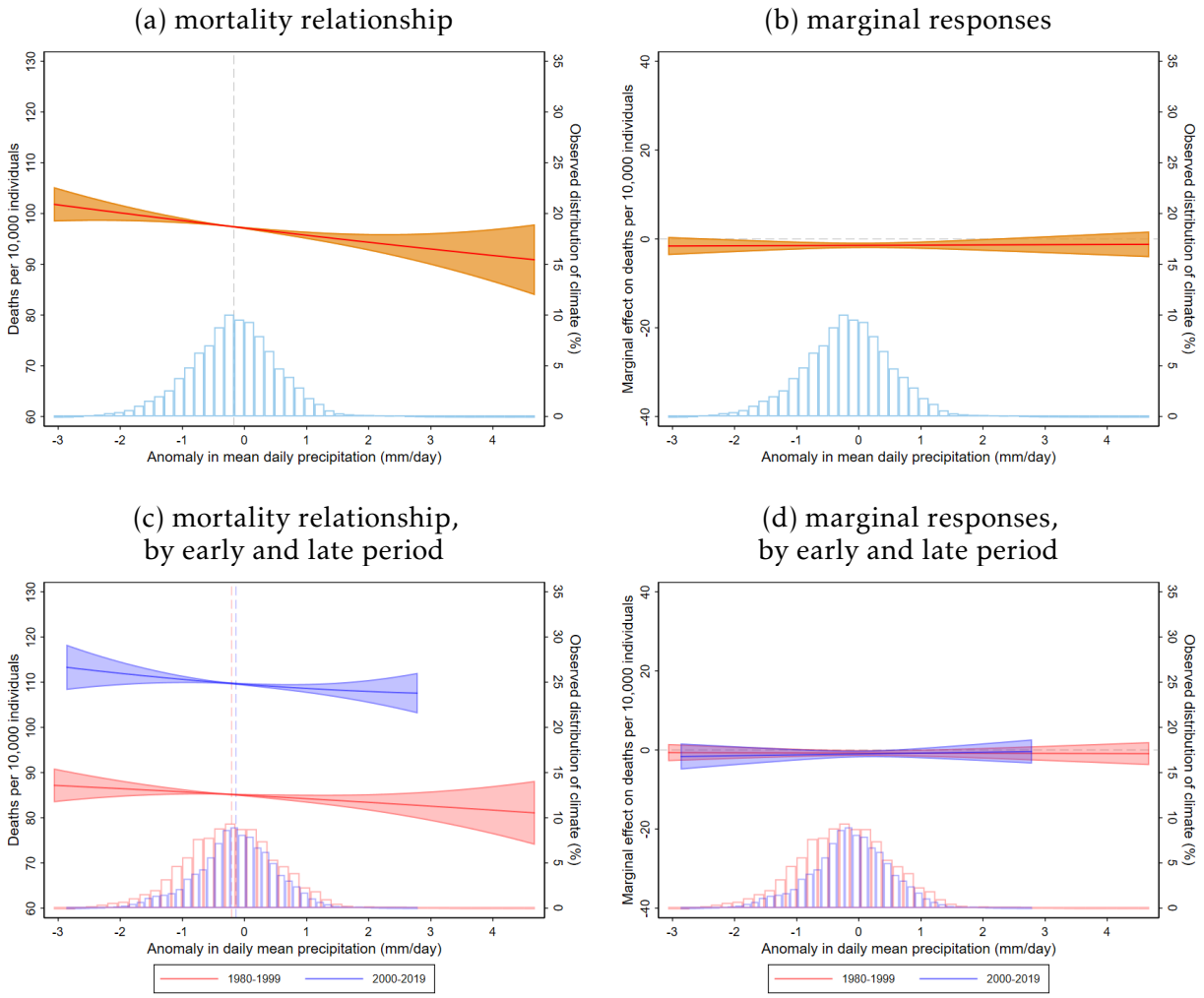

Notes: Figure shows the relationship between mortality and mean daily precipitation as estimated by the quadratic specification in equation 4. Panel (a) plots predicted mortality for precipitation anomalies ranging from the minimum to the maximum in the estimation sample, and panel (b) plots the marginal responses.The empirical distribution of the anomalies observed over the study period is shown in the histogram in light blue. Panel (c) and (d) plot the predicted mortality and the marginal responses separately for the early (1980-1999) and late (2000-2019) periods of climate change, with the empirical distribution of climate anomalies in each period shown in histograms. The dotted vertical lines mark the mean anomaly in the full sample and in each sub-period. 95% confidence intervals from standard errors clustered at the level of municipalities are shown for the predicted mortality and marginal responses.

levels of humidity. Specifically, reducing humidity by 1 percentage point at low levels (e.g., 2 pp below climatology) would decrease mortality in Kansai and Shikoku by 1.90-2.03 deaths per 10,000 individuals per year, whereas in Hokkaido, the humidity reduction would increase mortality by 1.48 deaths per 10,000 individuals per year.

In Figure 10, greater precipitation significantly reduces mortality in the northern regions of Hokkaido and Tohoku, and reduces mortality especially at high precipitation levels in the southern-central region of Kansai. However, as precipitation was lower than climatology in all three regions (by 0.09-0.13 mm/day in Hokkaido-Tohoku and by 0.38 mm/day in Kansai), the precipitation drops increased mortality by 0.29-0.38 deaths per 10,000 individuals per year in Hokkaido and Tohoku, and by 1.09 deaths per 10,000 individuals per year in Kansai.

3.3 Heterogeneity by climate

I next explore heterogeneous mortality responses across the baseline climate as characterized by the 30-year average of climate change indicators over the climatology period in 1951-1980. Figure 11 shows mortality responses to mean daily air temperature. Each mortality response curve is estimated from a separate regression focusing on municipalities above or below the median municipality of a given climate. At higher temperatures, the marginal response curve is steeper in municipalities that are warmer (panel a), wetter (panel d), more humid (panel c), as well as municipalities with greater humidity amplification (panel b) in the climatology baseline. These municipalities are primarily located in the southern-central and the southern regions, where the mortality responses are also larger (Figure 7). In contrast, in colder, dryer climates with low humidity amplification, the mortality responses to temperature are not statistically different from zero.

In Figure 12, the mortality responses to humidity amplification are larger in municipalities in a cold and humid climate (panel a and c) with low levels of humidity amplification (panel b) in the climatology baseline. These municipalities are primarily located in the

Figure 7: Mortality responses to mean daily air temperature, by regions

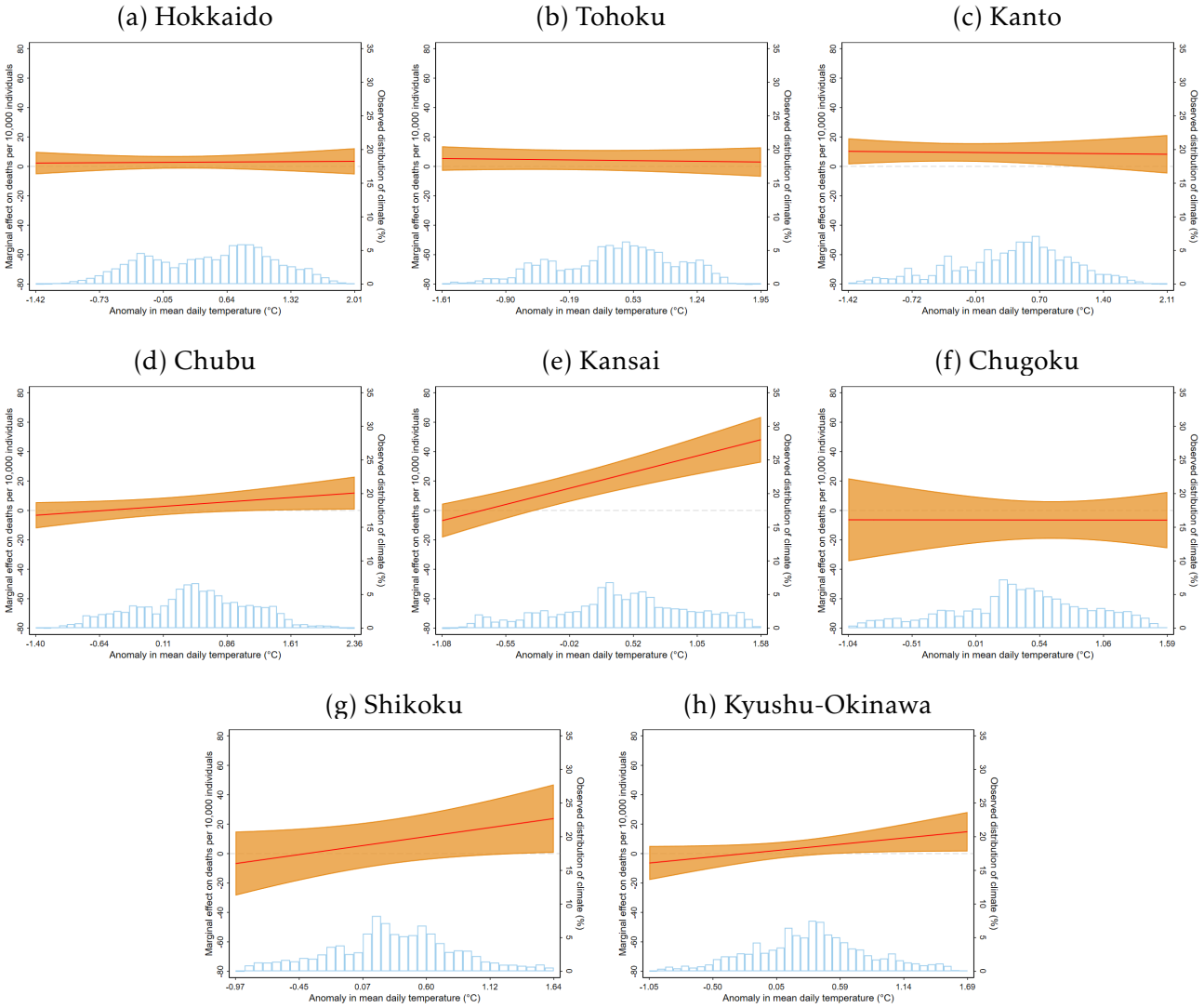

Notes: Figure shows the marginal responses to mean daily air temperature estimated from separate regressions across 8 regions in Japan. The empirical distribution of the anomalies observed in each region over the study period is shown in the histogram in light blue. The x-axis labels indicate the minimum and maximum values observed in the region as well as the 20th, 40th, 60th, 80th percentiles. 95% confidence intervals from standard errors clustered at the level of municipalities are shown for the marginal responses.

Figure 8: Mortality responses to humidity amplification, by regions

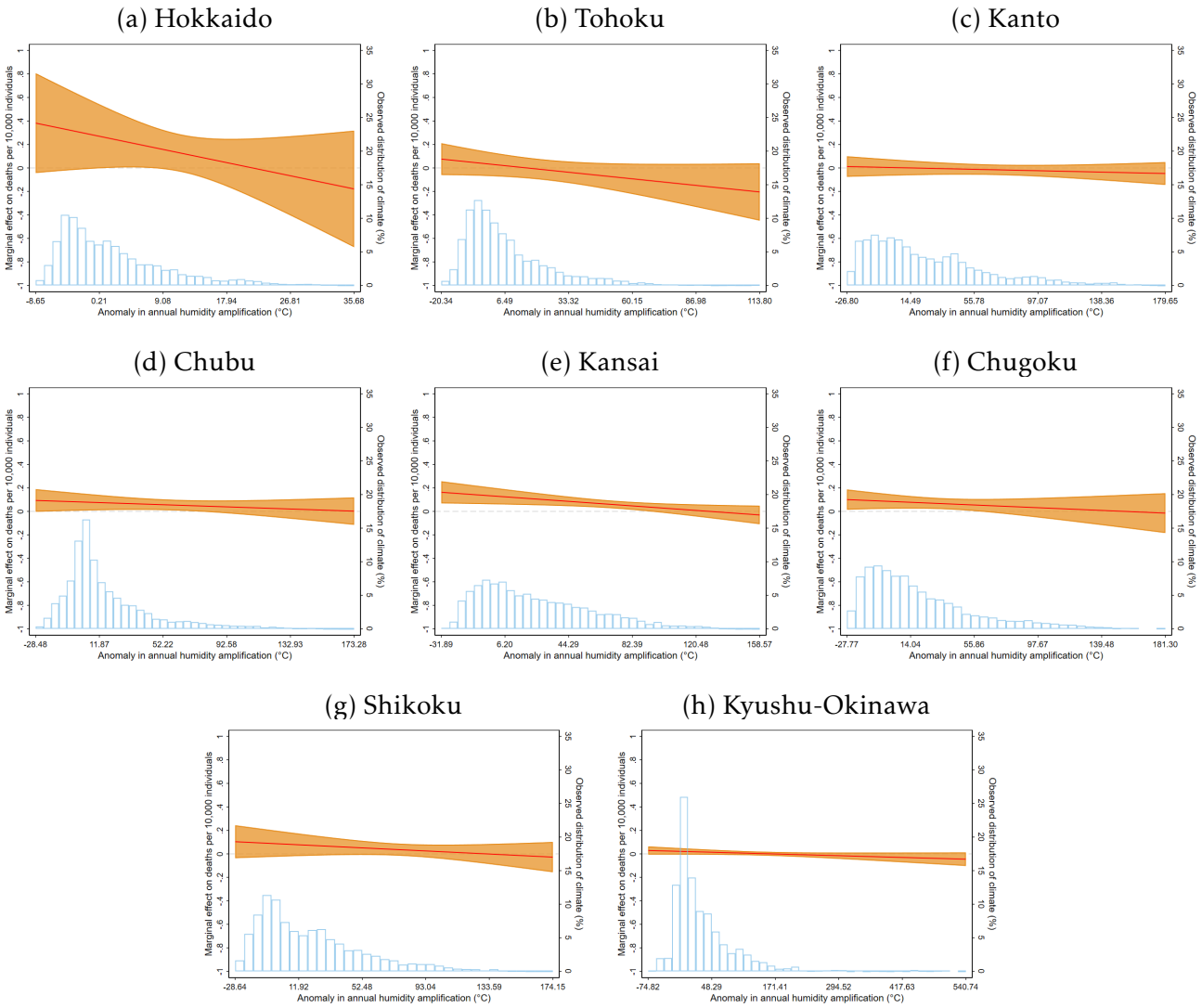

Notes: Figure shows the marginal responses to humidity amplification estimated from separate regressions across 8 regions in Japan. The empirical distribution of the anomalies observed in each region over the study period is shown in the histogram in light blue. The x-axis labels indicate the minimum and maximum values observed in the region as well as the 20th, 40th, 60th, 80th percentiles. 95% confidence intervals from standard errors clustered at the level of municipalities are shown for the marginal responses.

Figure 9: Mortality responses to mean daily relative humidity, by regions

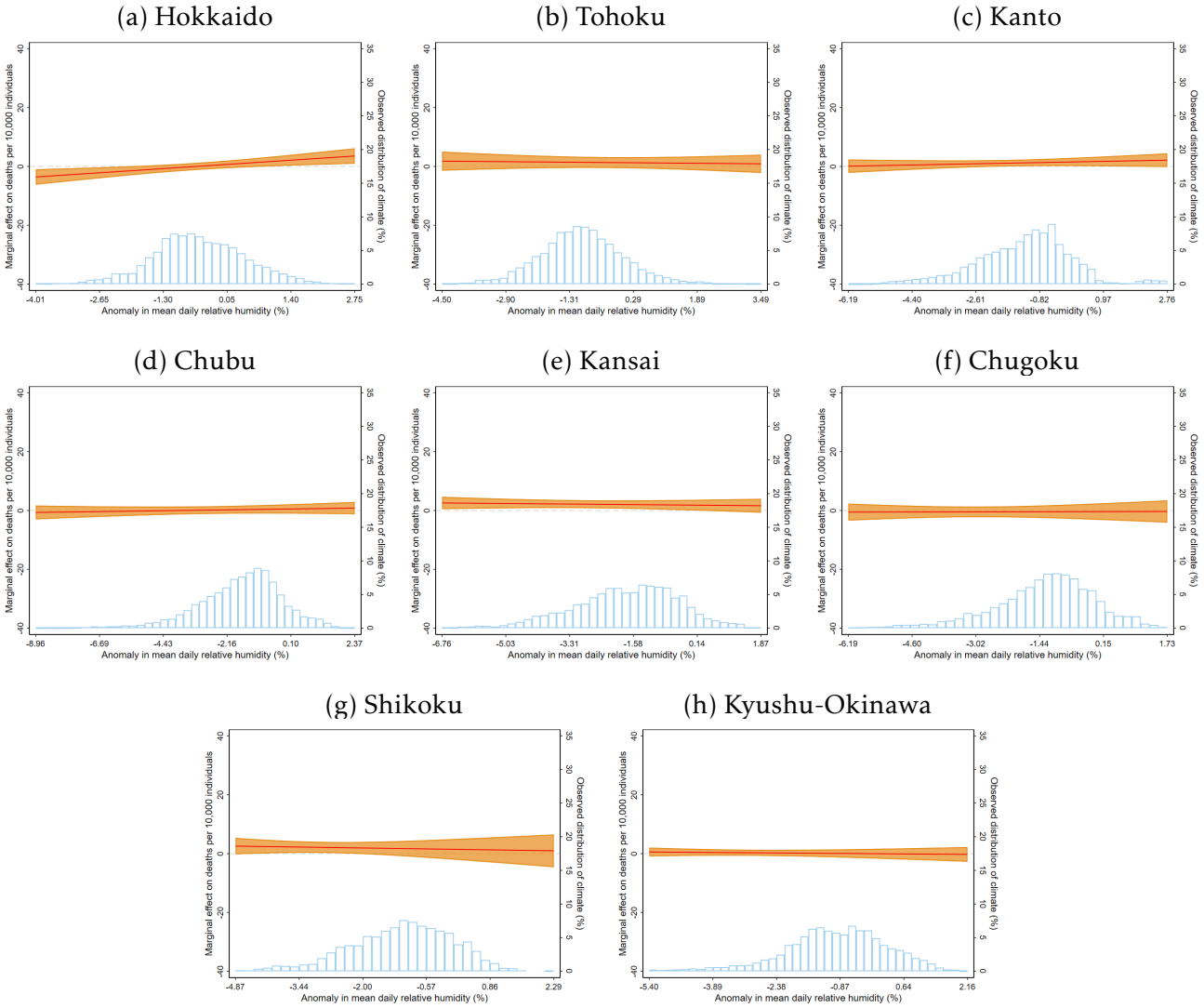

Notes: Figure shows the marginal responses to mean daily relative humidity estimated from separate regressions across 8 regions in Japan. The empirical distribution of the anomalies observed in each region over the study period is shown in the histogram in light blue. The x-axis labels indicate the minimum and maximum values observed in the region as well as the 20th, 40th, 60th, 80th percentiles. 95% confidence intervals from standard errors clustered at the level of municipalities are shown for the marginal responses.

Figure 10: Mortality responses to mean daily precipitation, by regions

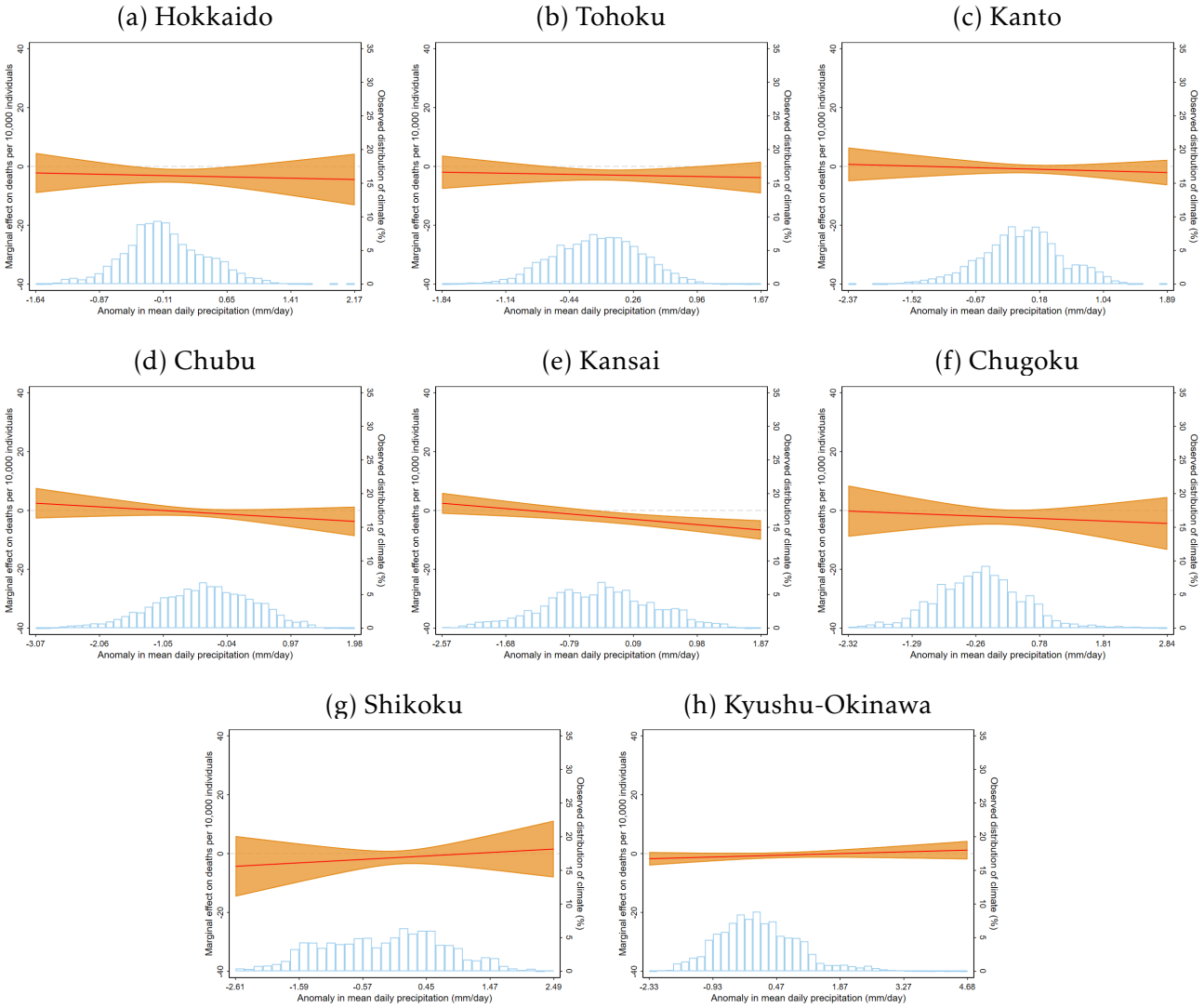

Notes: Figure shows the marginal responses to mean daily precipitation estimated from separate regressions across 8 regions in Japan. The empirical distribution of the anomalies observed in each region over the study period is shown in the histogram in light blue. The x-axis labels indicate the minimum and maximum values observed in the region as well as the 20th, 40th, 60th, 80th percentiles. 95% confidence intervals from standard errors clustered at the level of municipalities are shown for the marginal responses.

northern regions with low temperatures, low humidity amplification, and high relative humidity, where the mortality responses to humidity amplification are also larger (Figure 8). The mortality responses in warm, dry climates and climates with high levels of humidity amplification are not statistically different from zero. In panel (d), the mortality responses are larger in municipalities with greater precipitation, although the difference is only marginally significant.

In Figure 13, the mortality responses to relative humidity are larger in municipalities in colder climates with low levels of humidity amplification (panel a and b). In warmer climates with high levels of humidity amplification, the mortality responses are not statistically different from zero. In panel (c) and (d), the mortality responses do not differ significantly across humidity or precipitation levels in the baseline climate.

In Figure 14, mortality decreases significantly with greater precipitation in municipalities that are colder (panel a), more humid (panel c), and have lower levels of humidity amplification (panel b). These municipalities are concentrated in the northern regions, where lower precipitation levels under climate change would lead to larger increases in mortality. In panel (d), mortality responses to precipitation do not differ significantly across high and low precipitation levels in the baseline climate.

3.4 Heterogeneity by socio-economic characteristics

Figures 15 to 18 explore heterogeneous mortality responses across the socio-economic characteristics of municipalities. In Figure 15, the mortality responses to temperature are larger in urban municipalities (panel a), densely populated municipalities (panel b), and higher-income municipalities (panels c). Municipalities with higher agricultural income, however show larger mortality increases with temperature (panel d). Panels (e) and (f) contrast the mortality responses in ageing municipalities with higher shares of older individuals with those in non-ageing municipalities. While older individuals are more susceptible to the ill effects of extreme heat, the mortality responses are smaller

Figure 11: Mortality responses to mean daily air temperature, by climate

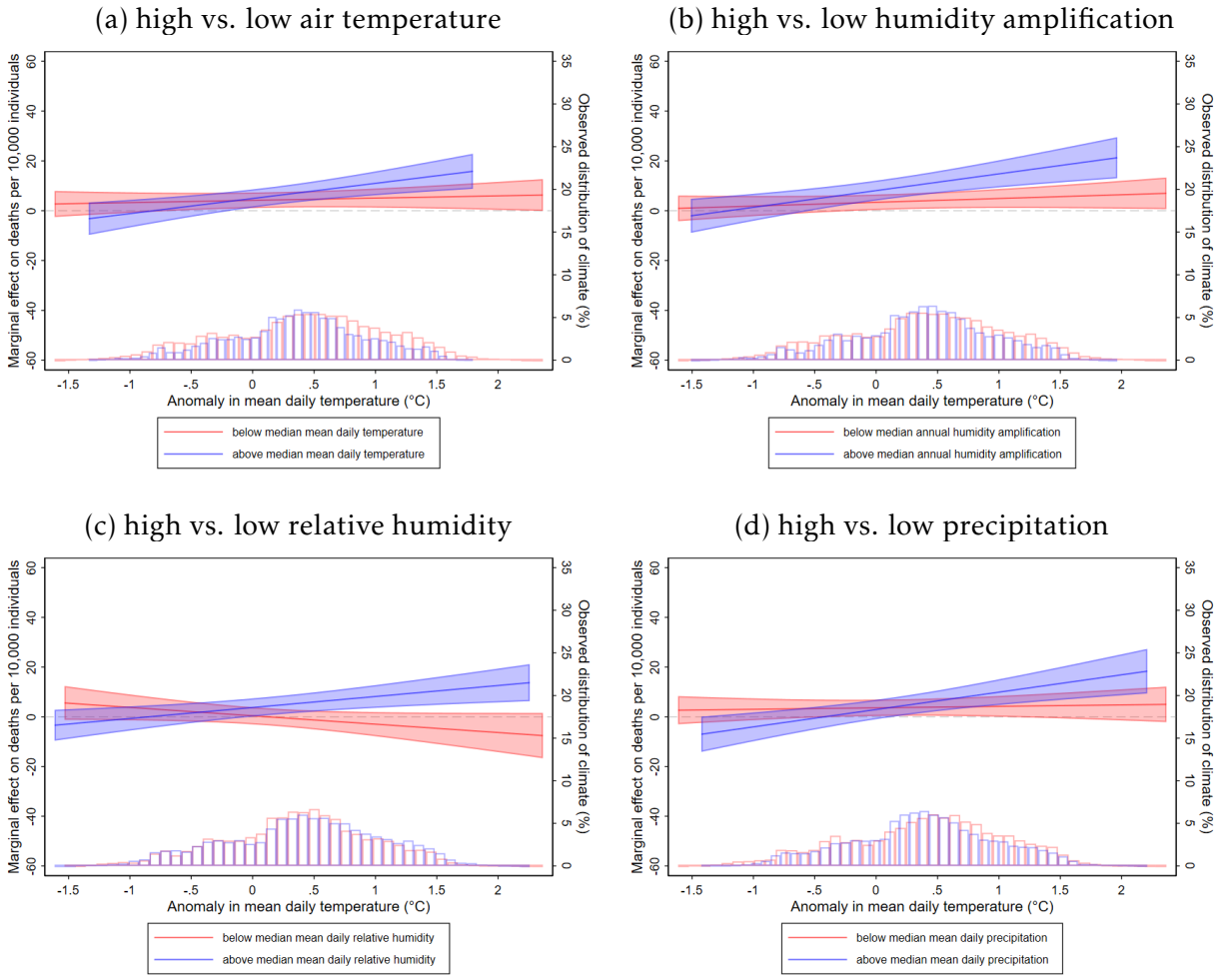

Notes: Figure shows the marginal responses to mean daily air temperature across the baseline climate, characterized by the 30-year average of the climate change indicators over the climatology period in 1951-1980. Each marginal response curve is estimated from a separate regression focusing on municipalities above or below the median municipality of a give climate, with the empirical distribution of climate anomalies observed in each sub-sample shown in histograms. 95% confidence intervals from standard errors clustered at the level of municipalities are shown for the marginal responses.

Figure 12: Mortality responses to humidity amplification, by climate

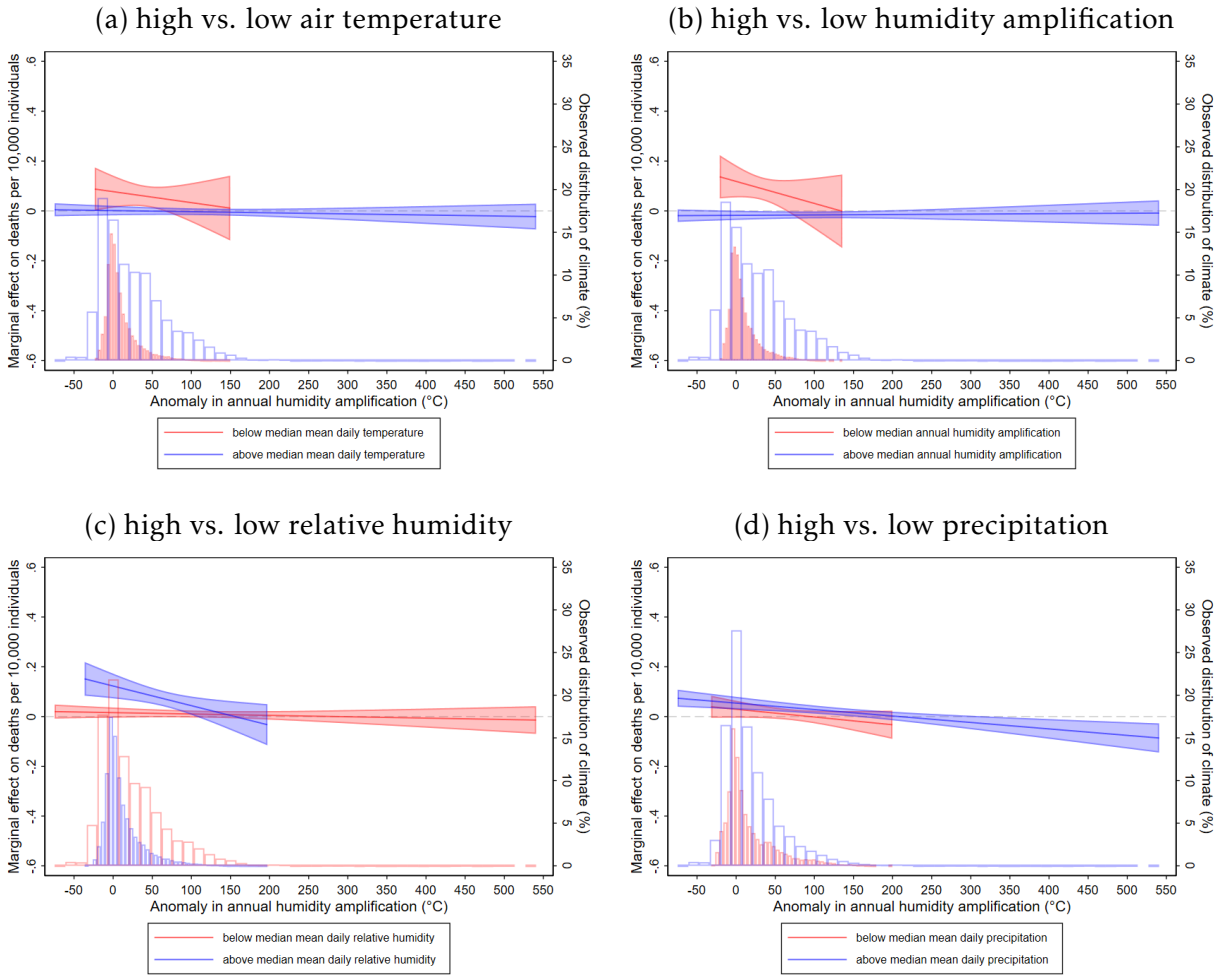

Notes: Figure shows the marginal responses to humidity amplification across across the baseline climate, characterized by the 30-year average of the climate change indicators over the climatology period in 1951-1980. Each marginal response curve is estimated from a separate regression focusing on municipalities above or below the median municipality of a give climate, with the empirical distribution of climate anomalies observed in each sub-sample shown in histograms. 95% confidence intervals from standard errors clustered at the level of municipalities are shown for the marginal responses.

Figure 13: Mortality responses to mean daily relative humidity, by climate

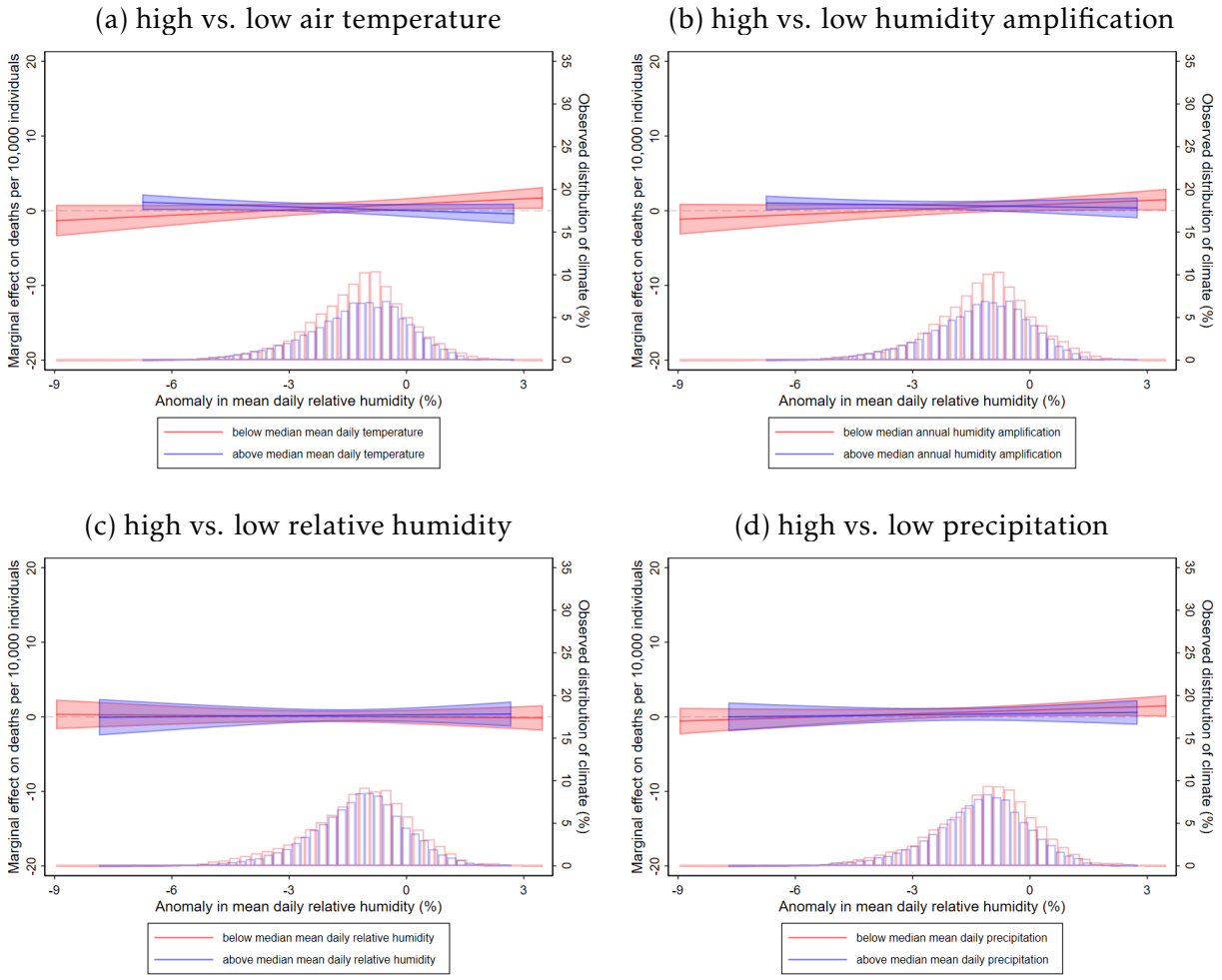

Notes: Figure shows the marginal responses to mean daily relative humidity across the baseline climate, characterized by the 30-year average of the climate change indicators over the climatology period in 1951-1980. Each marginal response curve is estimated from a separate regression focusing on municipalities above or below the median municipality of a give climate, with the empirical distribution of climate anomalies observed in each sub-sample shown in histograms. 95% confidence intervals from standard errors clustered at the level of municipalities are shown for the marginal responses.

Figure 14: Mortality responses to mean daily precipitation, by climate

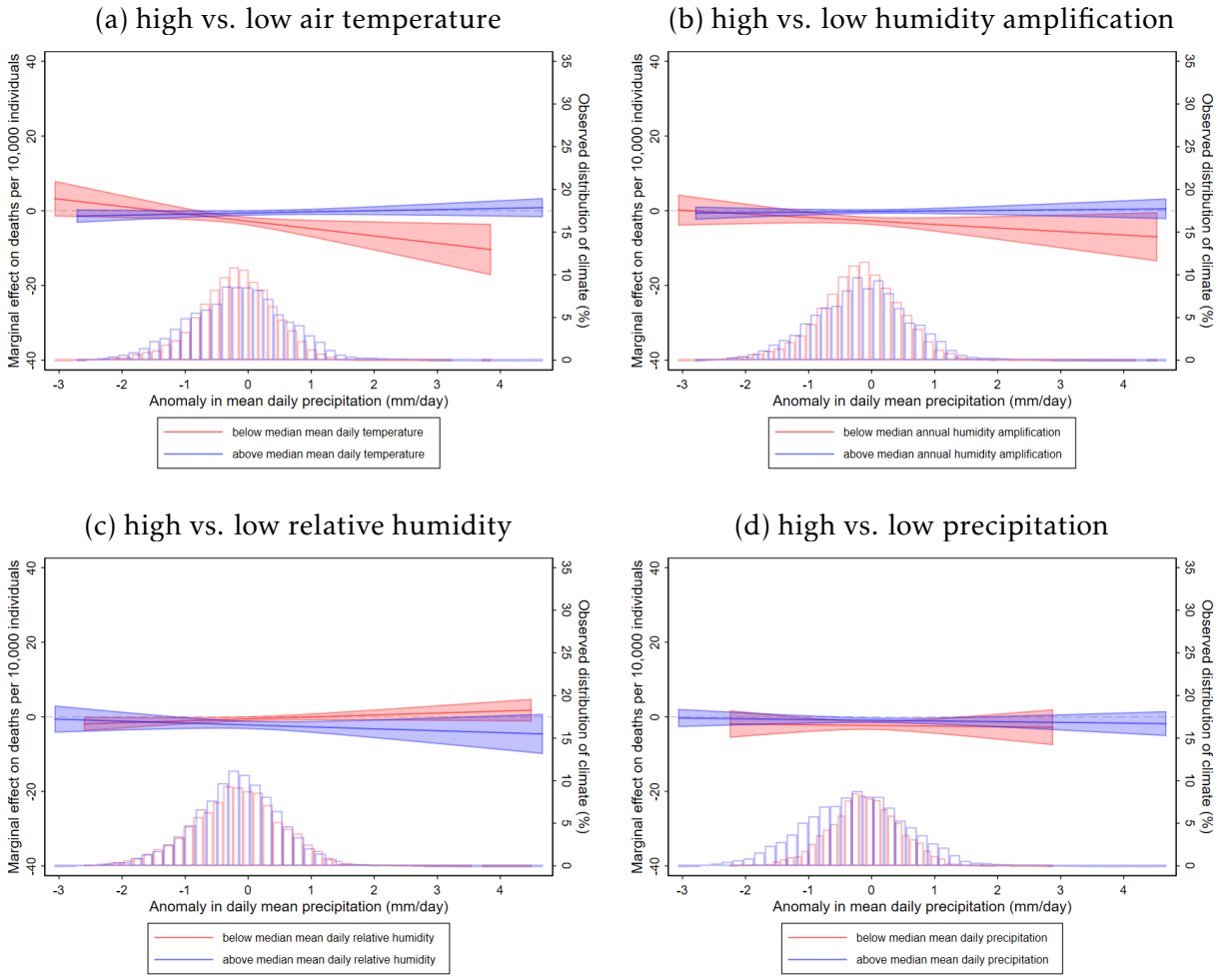

Notes: Figure shows the marginal responses to mean daily precipitation across the baseline climate, characterized by the 30-year average of the climate change indicators over the climatology period in 1951-1980. Each marginal response curve is estimated from a separate regression focusing on municipalities above or below the median municipality of a give climate, with the empirical distribution of climate anomalies observed in each sub-sample shown in histograms. 95% confidence intervals from standard errors clustered at the level of municipalities are shown for the marginal responses.

in ageing municipalities in Japan over the study period, although the difference is only marginally significant.

In Figure 16, the mortality responses to humidity amplification are larger in rural municipalities (panel a) and higher-income municipalities (panel c). Municipalities with higher agricultural income, however, show smaller mortality increases with humidity amplification (panel d). Unlike the case with temperature, across ageing and non-ageing municipalities, the mortality responses to humidity amplification are larger in ageing municipalities with higher shares of older individuals (panel e and f).

In Figure 17, the mortality responses to relative humidity are larger in rural municipalities (panel a), less densely populated municipalities (panel b), and higher-income municipalities (panel c). Municipalities with higher agricultural income, however, show smaller mortality increases with humidity (panel d). In panel (e), mortality responses are larger in ageing municipalities with higher shares of individuals above age 60, although the difference is not statistically significant at older ages in panel (f).

In Figure 18, greater precipitation significantly reduces mortality in rural municipalities, whereas in urban municipalities, the mortality effect is precisely estimated as zero across the precipitation anomalies observed in sample (panel a). In low-income municipalities, low precipitation extremes increase mortality (panel c), whereas in municipalities with low agricultural income, high precipitation extremes decrease mortality significantly (panel d). In panel (e) and (f), differences in mortality responses across ageing and non-ageing municipalities are not statistically significant.

4 Discussion

Using data across 1718 Japan municipalities in 1980-2019, this paper identifies the leading climate drivers of mortality in Japan and quantifies the climate-mortality relationship based on model specifications selected by LASSO. While the previous literature has mainly

Figure 15: Mortality responses to mean daily air temperature, by socio-economic characteristics

(a) rural vs. urban

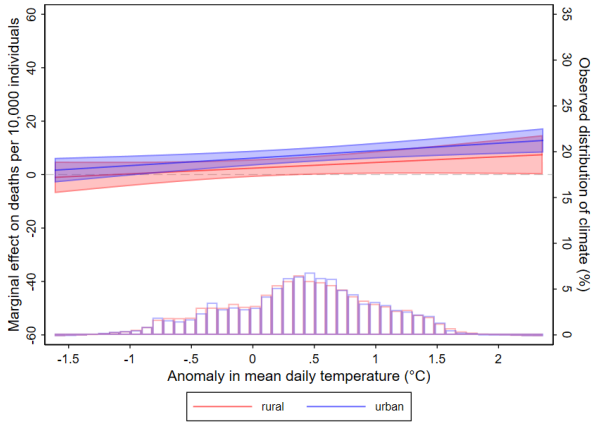

(b) high vs. low population density

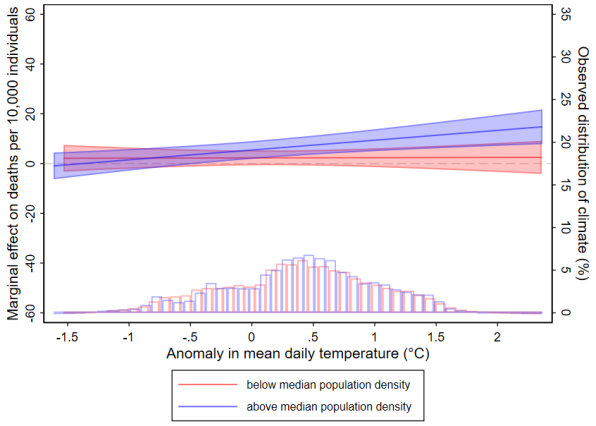

(c) high vs. low p.c. income

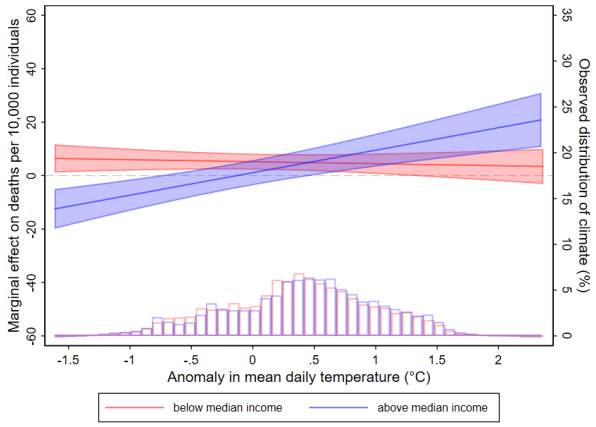

(d) high vs. low p.c. agricultural income

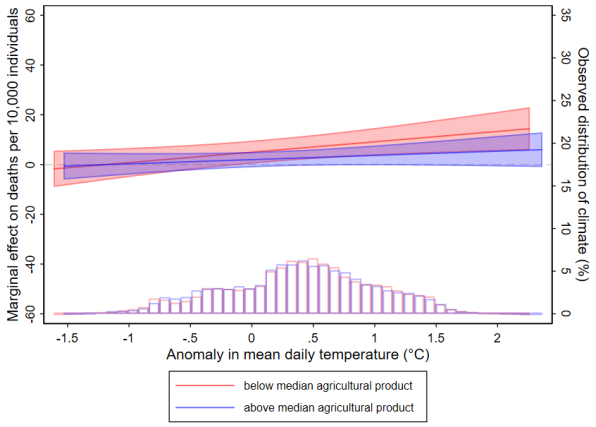

(e) high vs. low share above age 60

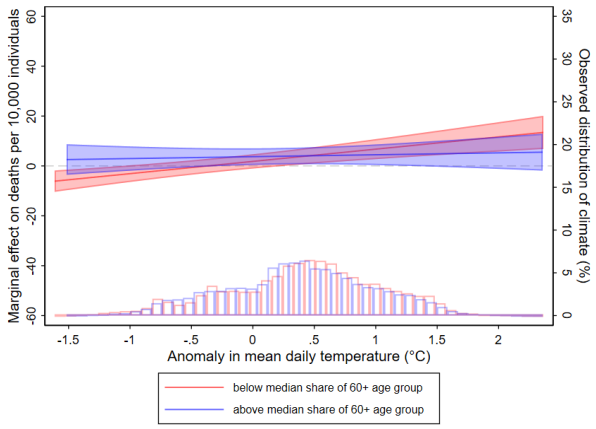

(f) high vs. low share above age 80

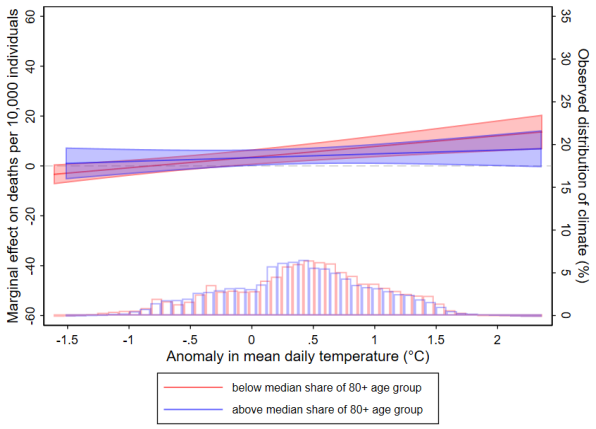

Notes: Figure shows the marginal responses to mean daily air temperature across socio-economic characteristics. Each marginal response curve is estimated from a separate regression focusing on municipalities above or below the median municipality of a give characteristic, with the empirical distribution of climate anomalies observed in each sub-sample shown in histograms. 95% confidence intervals from standard errors clustered at the level of municipalities are shown for the marginal responses.

Figure 16: Mortality responses to humidity amplification, by socio-economic characteristics

(a) rural vs. urban

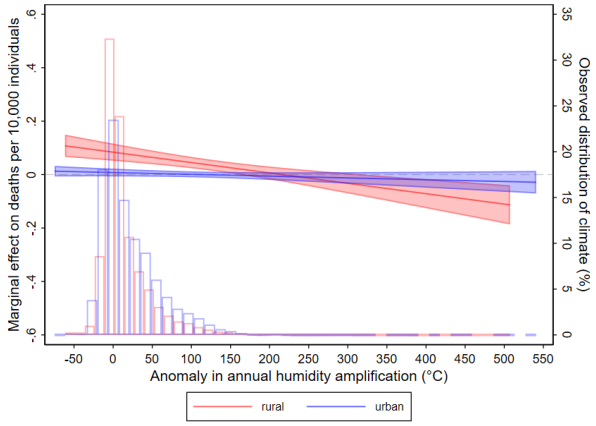

(b) high vs. low population density

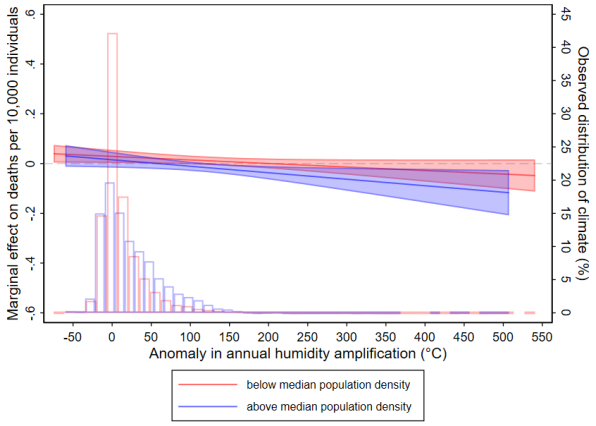

(c) high vs. low p.c. income

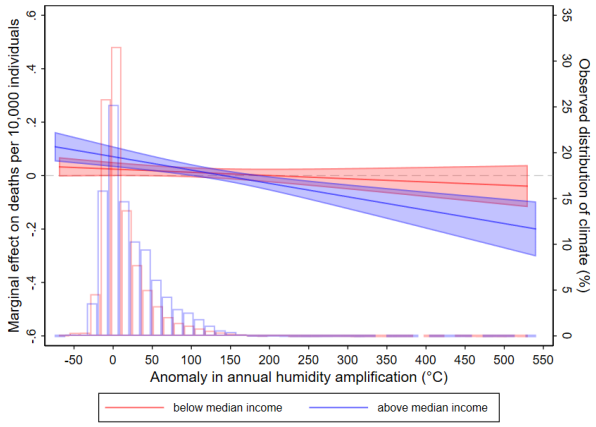

(d) high vs. low p.c. agricultural income

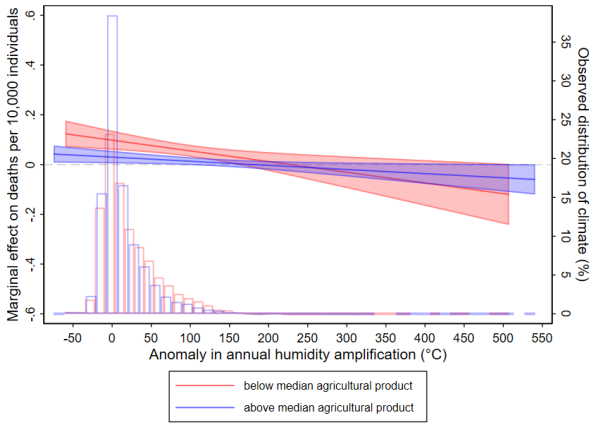

(e) high vs. low share above age 60

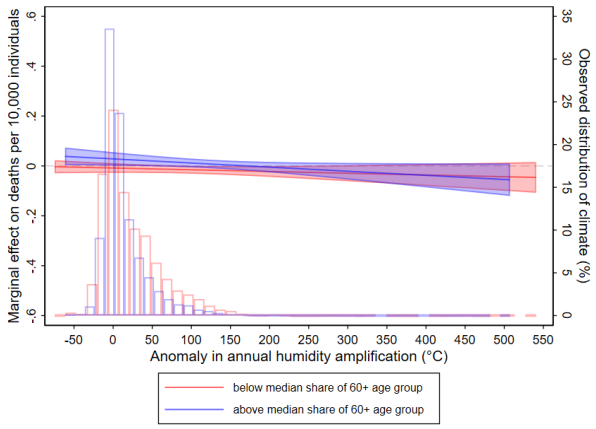

(f) high vs. low share above age 80

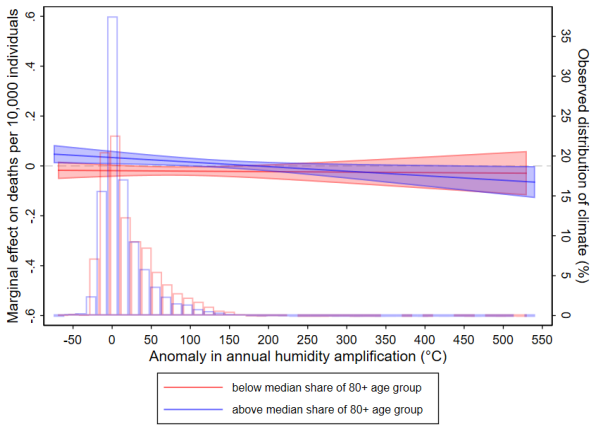

Notes: Figure shows the marginal responses to humidity amplification across socio-economic characteristics. Each marginal response curve is estimated from a separate regression focusing on municipalities above or below the median municipality of a give characteristic, with the empirical distribution of climate anomalies observed in each sub-sample shown in histograms. 95% confidence intervals from standard errors clustered at the level of municipalities are shown for the marginal responses.

Figure 17: Mortality responses to mean daily relative humidity, by socio-economic characteristics

(a) rural vs. urban

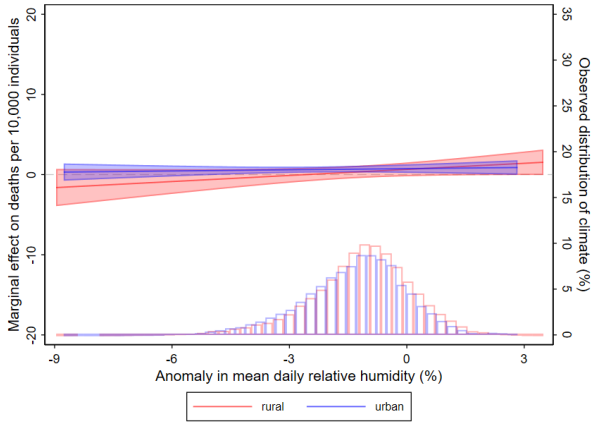

(b) high vs. low population density

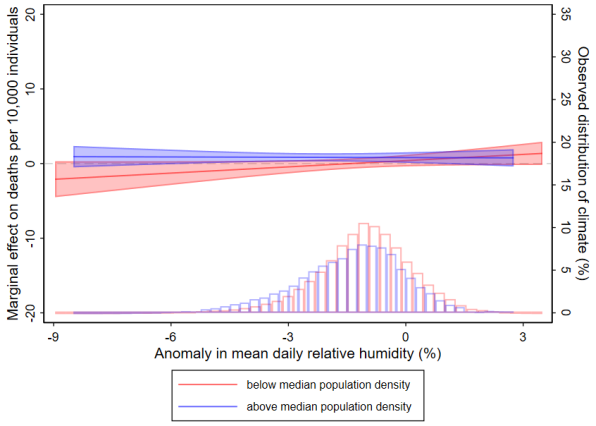

(c) high vs. low p.c. income

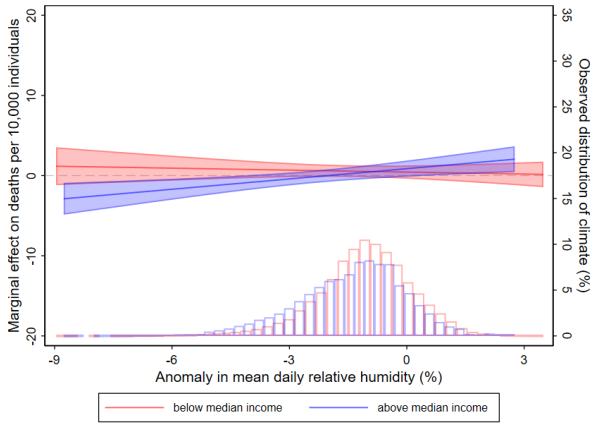

(d) high vs. low p.c. agricultural income

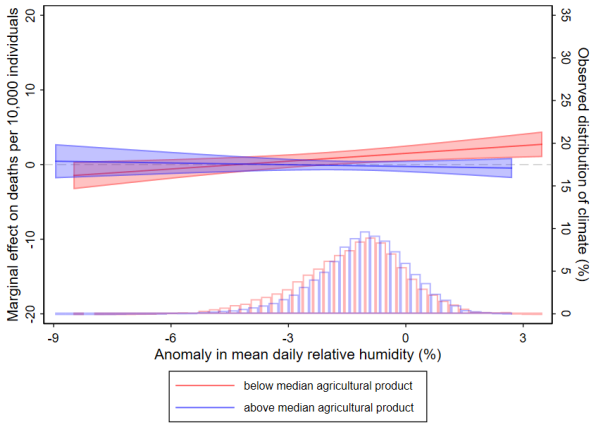

(e) high vs. low share above age 60

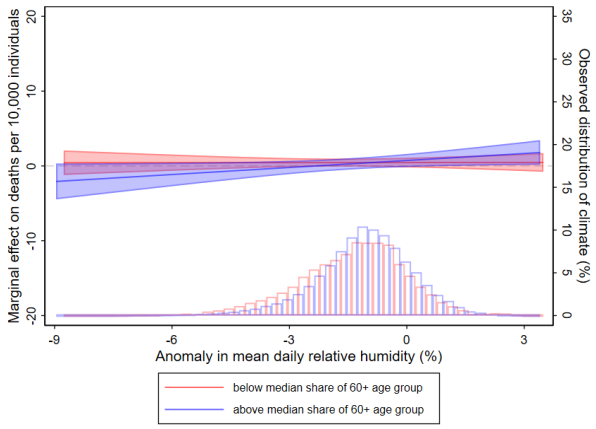

(f) high vs. low share above age 80

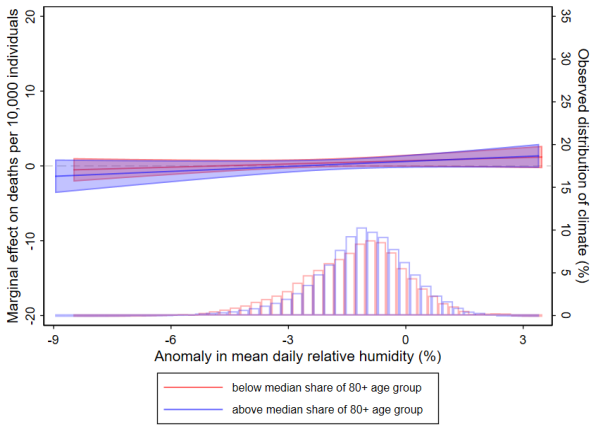

Notes: Figure shows the marginal responses to mean daily relative humidity across socio-economic characteristics. Each marginal response curve is estimated from a separate regression focusing on municipalities above or below the median municipality of a give characteristic, with the empirical distribution of climate anomalies observed in each sub-sample shown in histograms. 95% confidence intervals from standard errors clustered at the level of municipalities are shown for the marginal responses.

Figure 18: Mortality responses to mean daily precipitation, by socio-economic characteristics

(a) rural vs. urban

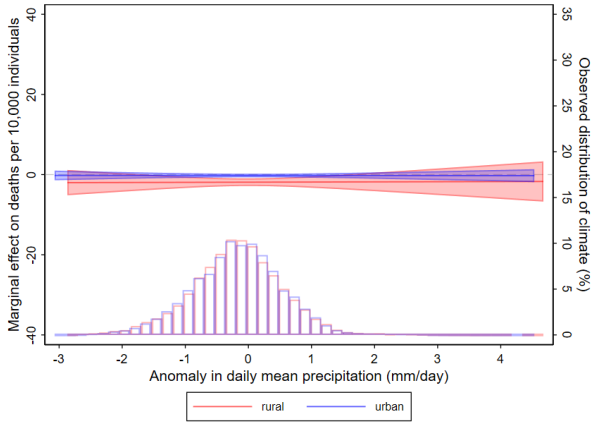

(b) high vs. low population density

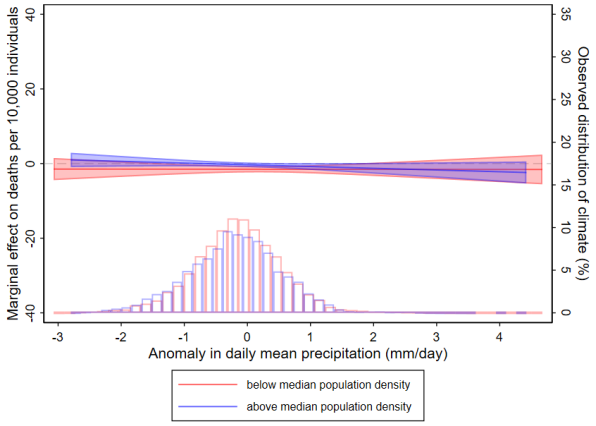

(c) high vs. low p.c. income

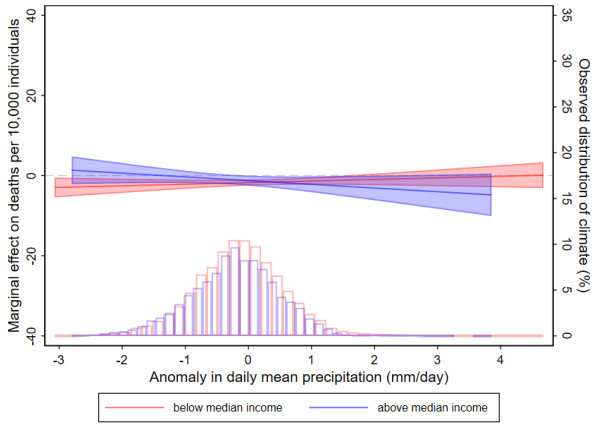

(d) high vs. low p.c. agricultural income

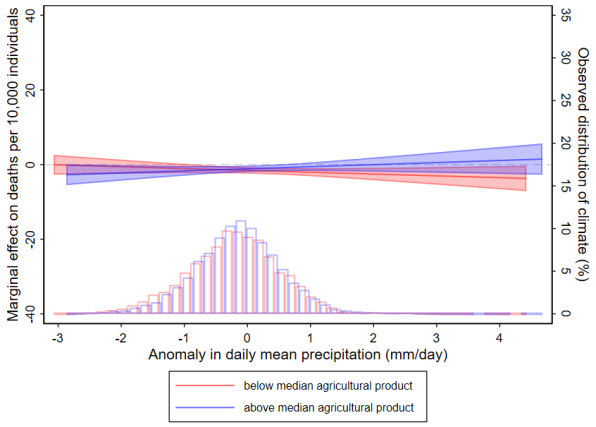

(e) high vs. low share above age 60

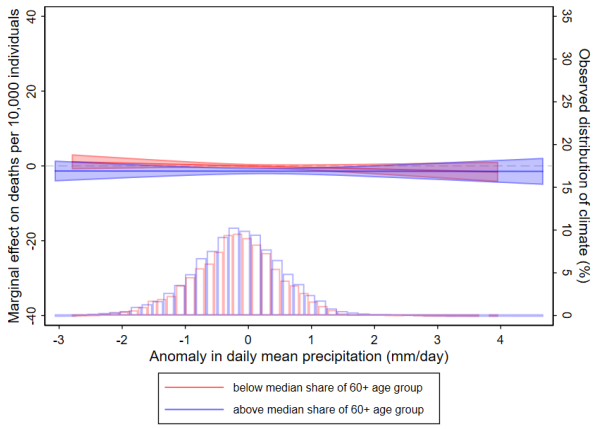

(f) high vs. low share above age 80

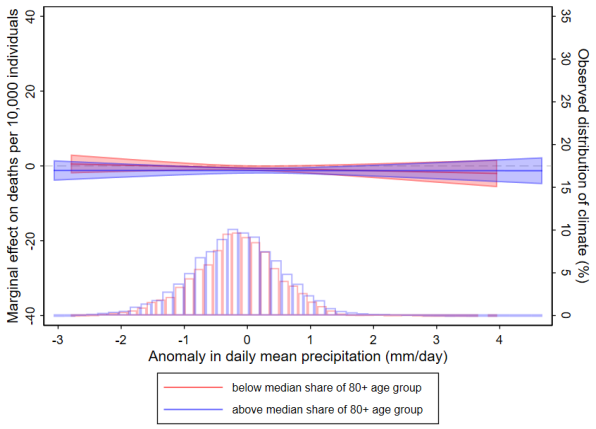

Notes: Figure shows the marginal responses to mean daily precipitation across socio-economic characteristics. Each marginal response curve is estimated from a separate regression focusing on municipalities above or below the median municipality of a give characteristic, with the empirical distribution of climate anomalies observed in each sub-sample shown in histograms. 95% confidence intervals from standard errors clustered at the level of municipalities are shown for the marginal responses.

focused on temperature as the key driver of climate-related deaths, the empirical analysis in this paper reveals that, in addition to temperature, relative humidity, precipitation, and humidity amplification in heat-and-humidity extremes all have significant impacts on mortality. Specifically, consistent with the previous literature, the relationship between temperature and mortality is highly non-linear, with mortality rising sharply with temperature in the heat extremes. For relative humidity, I find a similar non-linear relationship with greater mortality responses at both high and low extremes of relative humidity.

Figure 19 shows the cumulative mortality effect of climate change across 1718 municipalities in Japan. Relative to mortality under the climatology mean, the mortality increase due to observed weather anomalies in a year is constructed applying region-specific estimates of the climate-mortality relationship in equation 4, and the sum of the yearly mortality effects over the study period gives the cumulative mortality from climate change. Across Japan, the average municipality experienced a cumulative mortality of 120 deaths per 10,000 individuals from climate change over the study period. The largest mortality increases are concentrated in the southern-central and central regions of Kansai, Shikoku, and Chubu, where cumulative mortality averaged over 420 deaths per 10,000 individuals in Kansai and 120-150 deaths per 10,000 individuals in Shikoku and Chubu. The smallest mortality increases are concentrated in the northern region of Tohoku and the southern region of Chugoku, where more than 60% of the municipalities in fact experienced lower mortality with climate change over the study period.

Figure 20 shows the cumulative mortality effect across the climate change indicators. In panel (a), rising air temperature is the leading driver of climate-related deaths in Japan, with the average municipality experiencing a cumulative mortality of 129 deaths per 10,000 individuals from heat over the study period. The largest mortality effects are concentrated in Kansai (455 deaths per 10,000 individuals), Shikoku (146 deaths per 10,000 individuals), and the densely populated Kanto region (140 deaths per 10,000 individuals). By contrast, cumulative mortality from heat was much smaller in the northern regions of

Hokkaido and Tohoku (49-55 deaths per 10,000 individuals) and in fact decreased in the southern region of Chugoku by 99 deaths per 10,000 individuals over the study period.

In panel (b), humidity amplification increased mortality primarily in the southern-central regions of Kansai, Chubu, Shikoku, and Chugoku. In these regions, humidity amplification increased cumulative mortality by 43-93 deaths per 10,000 individuals in the average municipality, with especially large mortality increases (93 deaths per 10,000 individuals) in Kansai. In the northernmost Hokkaido and the southernmost Kyushu-Okinawa regions, humidity amplification increased mortality by a smaller 8-11 deaths per 10,000 individuals. Across Japan, the average municipality experienced a cumulative mortality of 26 deaths per 10,000 individuals from humidity amplification over the study period.

In panel (c), reductions in relative humidity overall decreased mortality in Japan, with the average municipality experiencing lower mortality by 43 deaths per 10,000 individuals over the study period. Larger mortality reductions are concentrated in Kansai (141 deaths per 10,000 individuals), Shikoku (77 deaths per 10,000 individuals), and the central and northern regions of Kanto and Tohoku (56-60 deaths per 10,000 individuals). In Hokkaido and Chugoku, however, relative humidity increased mortality by 13-23 deaths per 10,000 individuals over the study period.

In panel (d), reductions in precipitation overall increased mortality in Japan, with the average municipality experiencing higher mortality by 7 deaths per 10,000 individuals over the study period. Larger mortality increases are concentrated in Shikoku (35 deaths per 10,000 individuals) and in the regions of Hokkaido, Tohoku, and Kansai (9-13 deaths per 10,000 individuals). In the central regions of Kanto and Chubu, the mortality increases from precipitation are much smaller (0.12 deaths per 10,000 individuals).

Across time periods, there has been little adaptation in the mortality responses to heat extremes, humidity extremes, or precipitation. The lack of adaptation to heat extremes runs counter to the finidings in , who shows that the diffusion of air conditioners in

the 1960s significantly reduced the mortality from heat extremes in the US. Focusing on a later period in 1980-2019, the lack of adaptation in Japan suggests that technology innovations may have played limited roles in mitigating the mortality responses to heat in more recent periods of climate change. Moreover, urban municipalities with higher population density and income in fact have greater mortality from heat than rural, less densely populated municipalities. As urban residents tend to be younger, more educated, and hence less vulnerable to heat-related health risks, the larger mortality responses in urban areas might be due to intensified heat exposure caused by densely built urban landscapes and anthropogenic heating, i.e., the urban heat island effect (Patz *et al.* 2005; Huang *et al.* 2023). With future population growths concentrated in large metropolitan areas in Japan and elsewhere, the exposure to urban heat extremes is projected to increase under future warming (Masselot *et al.* 2025; Gao *et al.* 2024) and pose serious challenges to health systems in cities around the world.

While mortality responses to heat and humidity extremes show little adaptation over time, mortality responses to humidity amplification are fully concentrated in the early period of climate change and are statistically insignificant in the later period. Colder municipalities with low humidity amplification in the climatology baseline show larger mortality responses. These results suggest that humidity amplification could be most lethal where it is least anticipated and where residents are ill-adapted to its health effects, but adaptation may occur over time due to increased physiological tolerance (Candas *et al.* 1979; Buono *et al.* 1998) or due to improved warning systems and protective measures against humid heat (Linares *et al.* 2020; Raymond *et al.* 2020). To the extent that occupational exposure among agricultural workers is an important contributor to the mortality responses in rural municipalities, adaptation strategies that implement strict workplace safety standards for outdoor workers (Kjellstrom *et al.*, 2016) can lower the mortality burden of humid heat stress in rural municipalities.

Figure 19: Cumulative mortality effect of climate change, 1980-2019

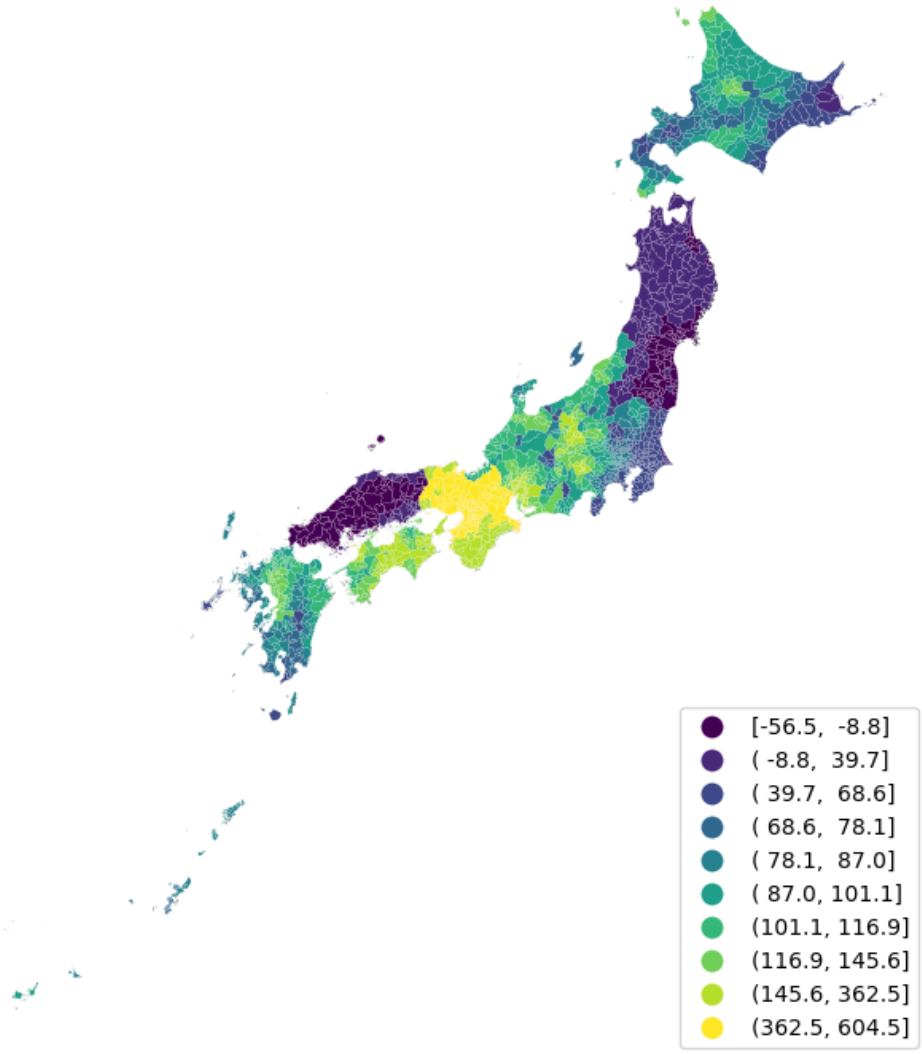

Notes: Figure shows the cumulative mortality effect of climate change across 1718 Japan municipalities over the study period in 1980-2019. Relative to mortality under the climatology mean, the mortality increase due to observed weather anomalies in a year is constructed applying region-specific estimates of the climate-mortality relationship in equation 4. The sum of yearly mortality effects gives the cumulative mortality effect of climate change. The color gradients correspond to the ten deciles in the distribution of cumulative mortality across municipalities.

Figure 20: Cumulative mortality effects of climate change indicators, 1980-2019

(a) air temperature

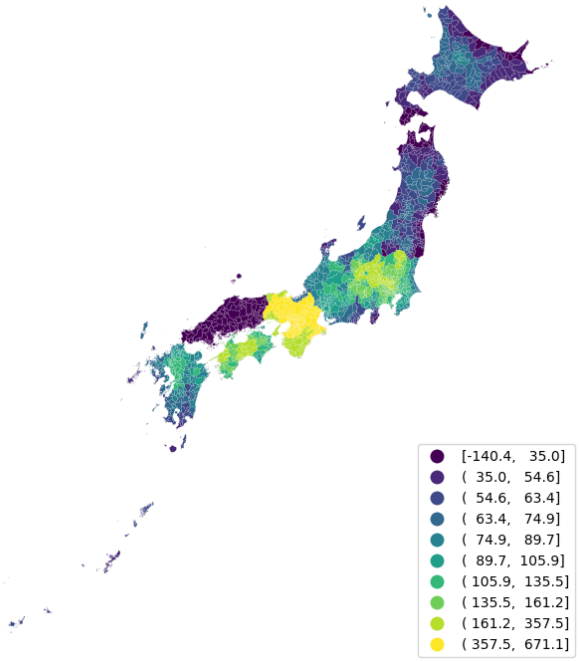

(b) humidity amplification

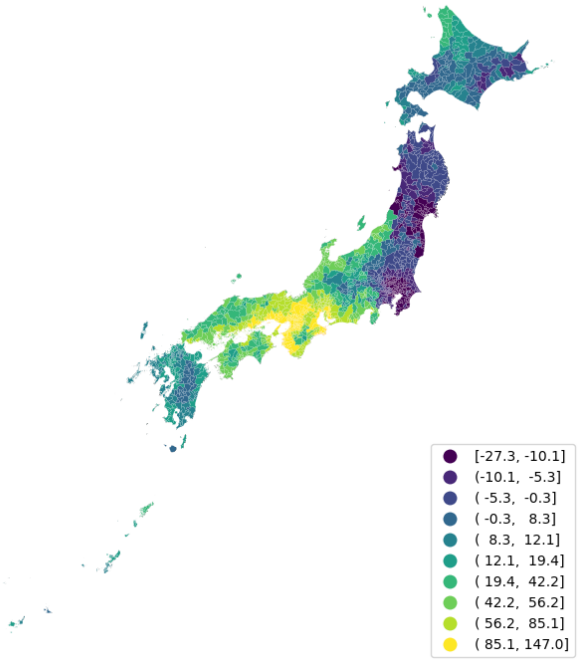

(c) relative humidity

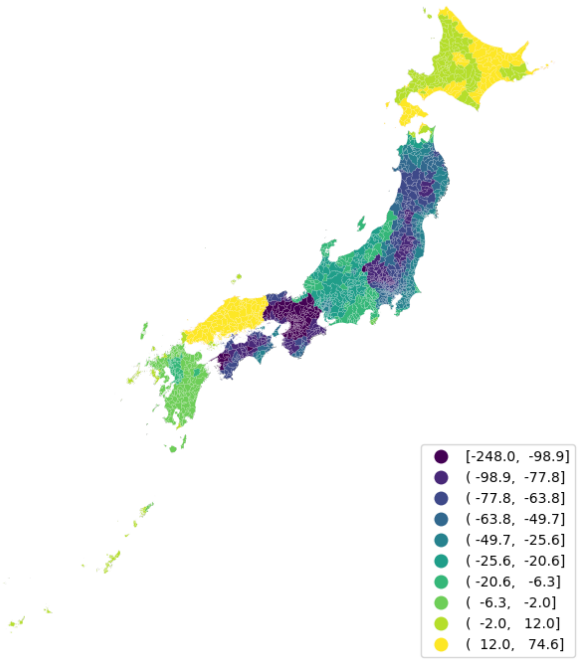

(d) precipitation

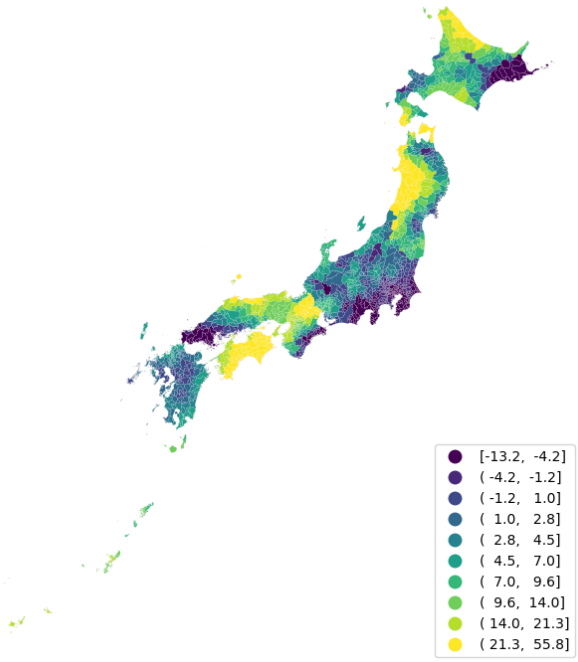

Notes: Figure shows the cumulative mortality effects of climate change indicators across 1718 Japan municipalities over the study period in 1980-2019. Relative to mortality under the climatology mean, the mortality increase due to observed weather anomalies is constructed for each year and climate change indicator applying region-specific estimates of the climate-mortality relationship in equation 4. The sum of yearly mortality effects gives the cumulative mortality effect of the climate change indicator. The color gradients correspond to the ten deciles in the distribution of cumulative mortality across municipalities.

Data Availability

The data used in this study .

Funding

The research is financially supported by the grants-in-aid for scientific research by early-career scientists (KAKENHI #23K12463), awarded by the Japan Society for the Promotion of Science. The financial support did not influence the data collection, research method, or the results obtained in this study.

Competing Interests

The author declares no competing interests.

References

AghaKouchak, A., Chiang, F., Huning, L. S., Love, C. A., Mallakpour, I., Mazdiyasni, O., Moftakhari, H., Papalexiou, S. M., Ragno, E. and Sadegh, M. (2020). Climate extremes and compound hazards in a warming world. *Annual Review of Earth and Planetary Sciences*, **48** (1), 519–548.

Allen, M., Dube, O. P., Solecki, W., Aragón-Durand, F., Cramer, W., Humphreys, S., Kainuma, M. *et al.* (2018). Special report: Global warming of 1.5 °C. *Intergovernmental Panel on Climate Change (IPCC)*, **677**, 393.

Armstrong McKay, D. I., Staal, A., Abrams, J. F., Winkelmann, R., Sakschewski, B., Loriani, S., Fetzer, I., Cornell, S. E., Rockström, J. and Lenton, T. M. (2022). Exceeding 1.5 °C global warming could trigger multiple climate tipping points. *Science*, **377** (6611), eabn7950.

Belloni, A., Chen, D., Chernozhukov, V. and Hansen, C. (2012). Sparse models and methods for optimal instruments with an application to eminent domain. *Econometrica*, **80** (6), 2369–2429.

—, Chernozhukov, V. and Hansen, C. (2014). Inference on treatment effects after selection among high-dimensional controls. *Review of Economic Studies*, **81** (2), 608–650.

—, —, — and Kozbur, D. (2016). Inference in high-dimensional panel models with an application to gun control. *Journal of Business & Economic Statistics*, **34** (4), 590–605.

Bevacqua, E., Schleussner, C.-F. and Zscheischler, J. (2025). A year above 1.5 °C signals that earth is most probably within the 20-year period that will reach the paris agreement limit. *Nature Climate Change*, pp. 1–4.

Bickel, P. J., Ritov, Y. and Tsybakov, A. B. (2009). Simultaneous analysis of lasso and dantzig selector.

Borrelli, P., Robinson, D. A., Panagos, P., Lugato, E., Yang, J. E., Alewell, C., Wuepper, D., Montanarella, L. and Ballabio, C. (2020). Land use and climate change impacts on global soil erosion by water (2015-2070). *Proceedings of the National Academy of Sciences*, **117** (36), 21994–22001.

Buono, M. J., Heaney, J. H. and Canine, K. M. (1998). Acclimation to humid heat lowers resting core temperature. *American Journal of Physiology-Regulatory, Integrative and Comparative Physiology*, **274** (5), R1295–R1299.

Burke, M., Hsiang, S. M. and Miguel, E. (2015). Global non-linear effect of temperature on economic production. *Nature*, **527** (7577), 235–239.

Candas, V., Libert, J. and Vogt, J. (1979). Influence of air velocity and heat acclimation on human skin wettedness and sweating efficiency. *Journal of applied physiology*, **47** (6), 1194–1200.

Carleton, T., Jina, A., Delgado, M., Greenstone, M., Houser, T., Hsiang, S., Hultgren, A., Kopp, R. E., McCusker, K. E., Nath, I. *et al.* (2022). Valuing the global mortality consequences of climate change accounting for adaptation costs and benefits. *The Quarterly Journal of Economics*, **137** (4), 2037–2105.

Colón-González, F. J., Sewe, M. O., Tompkins, A. M., Sjödin, H., Casallas, A., Rocklöv, J., Caminade, C. and Lowe, R. (2021). Projecting the risk of mosquito-borne diseases in a warmer and more populated world: a multi-model, multi-scenario intercomparison modelling study. *The Lancet Planetary Health*, **5** (7), e404–e414.

Cooper, M. W., Brown, M. E., Hochrainer-Stigler, S., Pflug, G., McCallum, I., Fritz, S., Silva, J. and Zvoleff, A. (2019). Mapping the effects of drought on child stunting. *Proceedings of the National Academy of Sciences*, **116** (35), 17219–17224.

Davenport, F. V., Burke, M. and Diffenbaugh, N. S. (2021). Contribution of historical precipitation change to us flood damages. *Proceedings of the National Academy of Sciences*, **118** (4), e2017524118.

Gao, S., Chen, Y., Chen, D., He, B., Gong, A., Hou, P., Li, K. and Cui, Y. (2024). Urbanization-induced warming amplifies population exposure to compound heatwaves but narrows exposure inequality between global north and south cities. *npj Climate and Atmospheric Science*, **7** (1), 154.

Hsiang, S. (2016). Climate econometrics. *Annual Review of Resource Economics*, **8** (1), 43–75.

Huang, W. T. K., Masselot, P., Bou-Zeid, E., Fatichi, S., Paschalis, A., Sun, T., Gasparrini, A. and Manoli, G. (2023). Economic valuation of temperature-related mortality attributed to urban heat islands in european cities. *Nature communications*, **14** (1), 7438.

Kjellstrom, T., Briggs, D., Freyberg, C., Lemke, B., Otto, M. and Hyatt, O. (2016). Heat, human performance, and occupational health: a key issue for the assessment of global climate change impacts. *Annual review of public health*, **37** (1), 97–112.

Knutson, T., Camargo, S. J., Chan, J. C., Emanuel, K., Ho, C.-H., Kossin, J., Mohapatra, M., Satoh, M., Sugi, M., Walsh, K. *et al.* (2020). Tropical cyclones and climate change assessment: Part ii: Projected response to anthropogenic warming. *Bulletin of the American Meteorological Society*, **101** (3), E303–E322.

Linares, C., Martinez, G., Kendrovski, V. and Diaz, J. (2020). A new integrative perspective on early warning systems for health in the context of climate change. *Environmental Research*, **187**, 109623.

Masselot, P., Mistry, M. N., Rao, S., Huber, V., Monteiro, A., Samoli, E., Stafoggia, M., de'Donato, F., Garcia-Leon, D., Ciscar, J.-C. *et al.* (2025). Estimating future heat-related and cold-related mortality under climate change, demographic and adaptation scenarios in 854 european cities. *Nature Medicine*, pp. 1–9.

Miller, S., Chua, K., Coggins, J. and Mohtadi, H. (2021). Heat waves, climate change, and economic output. *Journal of the European Economic Association*, **19** (5), 2658–2694.

Ortiz, A. M. D., Chua, P. L., Salvador Jr, D., Dyngeland, C., Albao Jr, J. D. G. and Abesamis, R. A. (2022). Impacts of tropical cyclones on food security, health and biodiversity. *Bulletin of the World Health Organization*, **101** (2), 152.

Osczevski, R. and Bluestein, M. (2005). The new wind chill equivalent temperature chart. *Bulletin of the American Meteorological Society*, **86** (10), 1453–1458.

Patz, J. A., Campbell-Lendrum, D., Holloway, T. and Foley, J. A. (2005). Impact of regional climate change on human health. *Nature*, **438** (7066), 310–317.

Raymond, C., Horton, R. M., Zscheischler, J., Martius, O., AghaKouchak, A., Balch, J., Bowen, S. G., Camargo, S. J., Hess, J., Kornhuber, K. *et al.* (2020). Understanding and managing connected extreme events. *Nature climate change*, **10** (7), 611–621.

Ridder, N. N., Pitman, A. J., Westra, S., Ukkola, A., Do, H. X., Bador, M., Hirsch, A. L., Evans, J. P., Di Luca, A. and Zscheischler, J. (2020). Global hotspots for the occurrence of compound events. *Nature communications*, **11** (1), 5956.

Steadman, R. G. (1979). The assessment of sultriness. part i: A temperature-humidity index based on human physiology and clothing science. *Journal of Applied Meteorology and Climatology*, **18** (7), 861–873.

Tank, A., Zwiers, F. and Zhang, X. (2009). Guidelines on analysis of extremes in a changing climate in support of informed decisions for adaptation. climate data and monitoring wcdmp-no. 72. *World Meteorological Organization, WMO-TD*, (1500).

Tibshirani, R. (1996). Regression shrinkage and selection via the lasso. *Journal of the Royal Statistical Society Series B: Statistical Methodology*, **58** (1), 267–288.

Von Uexkull, N., Croicu, M., Fjelde, H. and Buhaug, H. (2016). Civil conflict sensitivity to growing-season drought. *Proceedings of the National Academy of Sciences*, **113** (44), 12391–12396.

Zhang, X., Alexander, L., Hegerl, G. C., Jones, P., Tank, A. K., Peterson, T. C., Trewin, B. and Zwiers, F. W. (2011). Indices for monitoring changes in extremes based on daily temperature and precipitation data. *Wiley Interdisciplinary Reviews: Climate Change*, **2** (6), 851–870.

Zscheischler, J., Martius, O., Westra, S., Bevacqua, E., Raymond, C., Horton, R. M., van den Hurk, B., AghaKouchak, A., Jézéquel, A., Mahecha, M. D. *et al.* (2020). A typology of compound weather and climate events. *Nature reviews earth & environment*, **1** (7), 333–347.

A Appendix Figures

Figure A1: Correlation between the climate change indicators

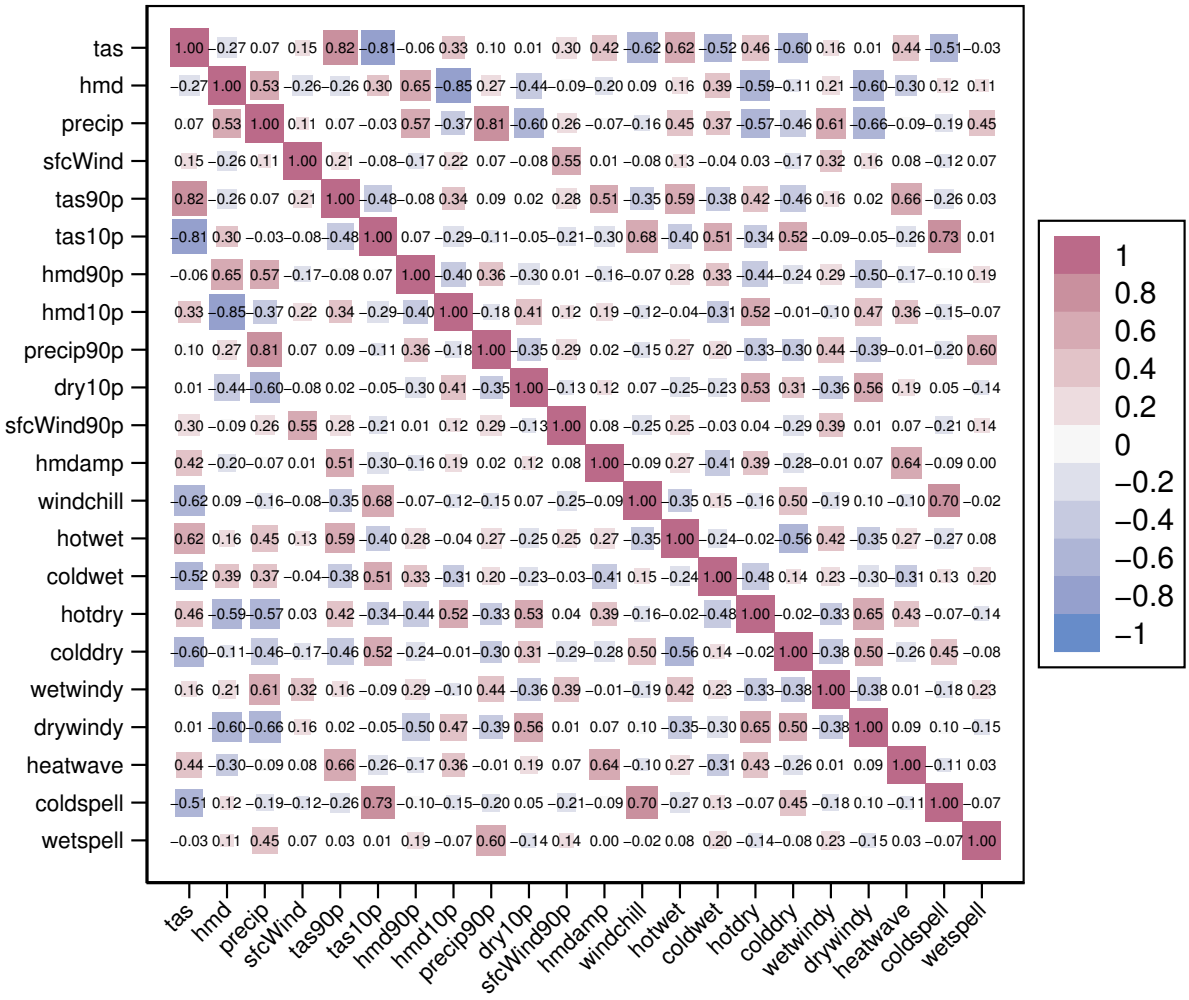

Notes: Figure plots the correlation coefficients across the climate change indicators based on a sample of 1718 Japan municipalities over the period in 1980-2019. The name and a short description of each indicator are shown in Table 1.

Figure A2: Climate change indicators across Japan municipalities, 1980-2019

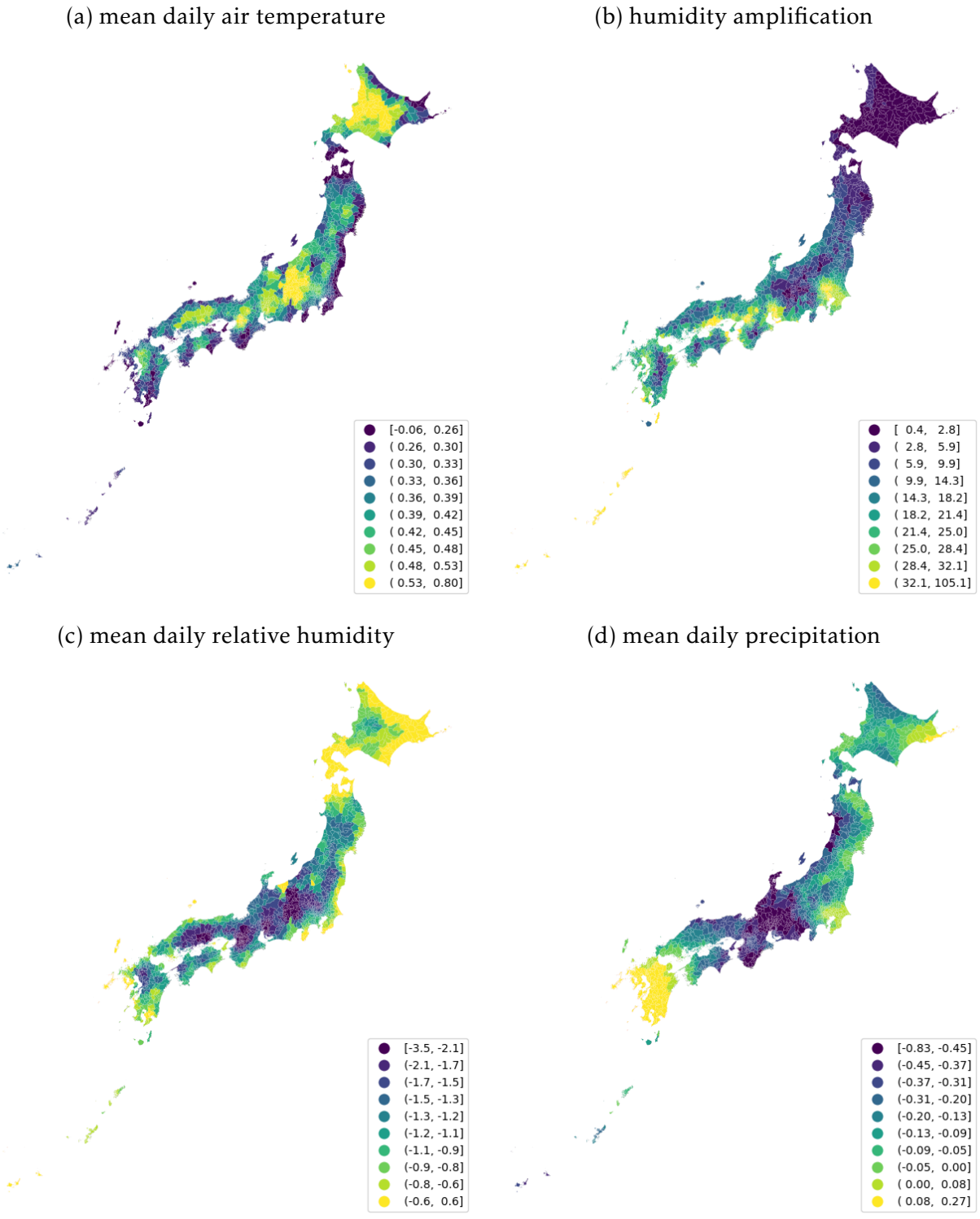

Notes: Figure shows the map of climate change indicators across 1718 municipalities in Japan. The climate change indicators are measured in anomalies and averaged over the study period (1980-2019) in the map. The color gradients correspond to the ten deciles in the empirical distribution of the indicator across municipalities.

Figure A3: Baseline climate across Japan municipalities, 1951-1980

(a) mean daily air temperature

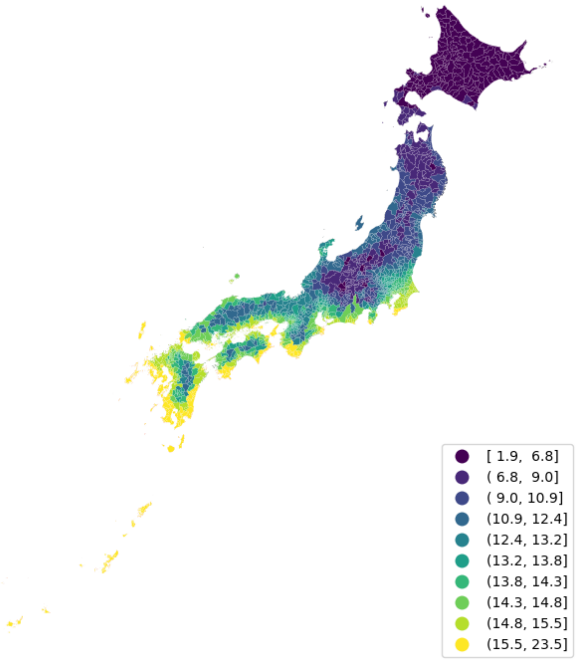

(b) humidity amplification

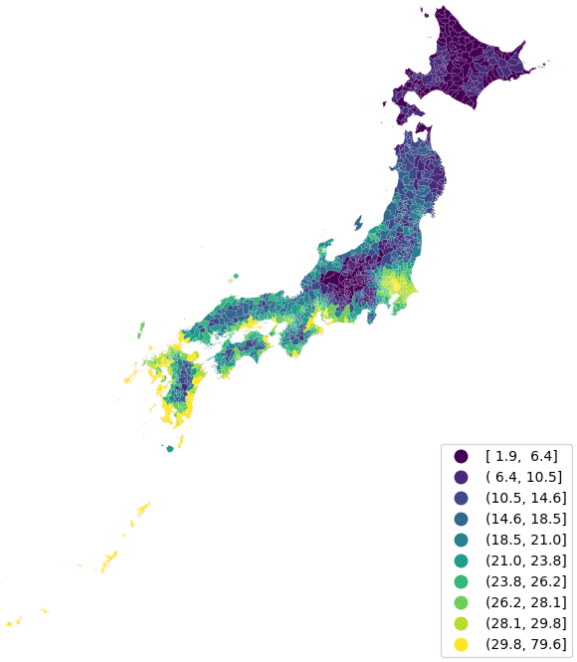

(c) mean daily relative humidity

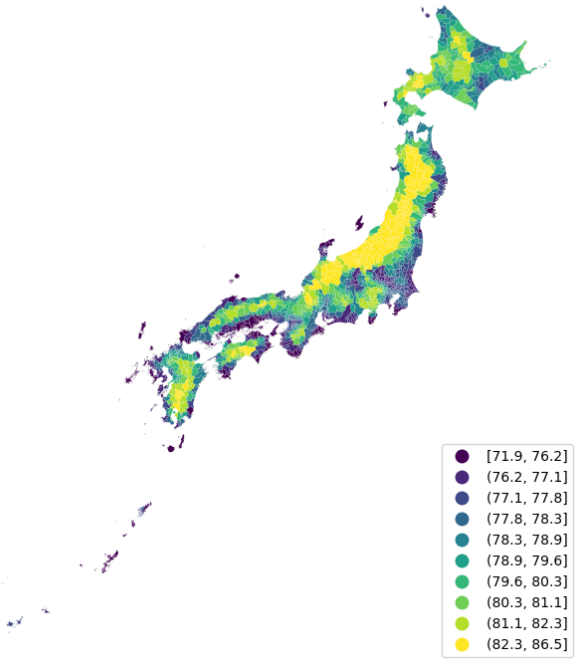

(d) mean daily precipitation

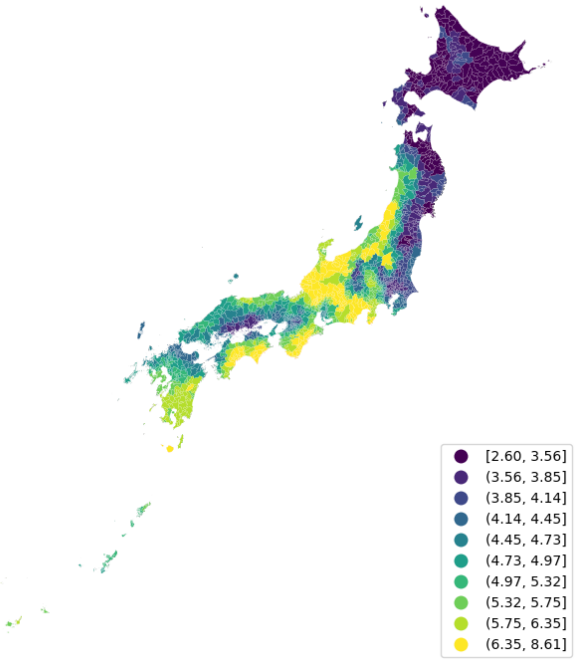

Notes: Figure shows the map of the baseline climate across 1718 municipalities in Japan. The baseline climate is characterized by the 30-year average of the climate change indicators over the climatology period in 1951-1980. The color gradients correspond to the ten deciles in the empirical distribution of climate across municipalities.